Carbocations as Electron Acceptors. Photoexcitation of the Charge-Transfer Complexes of Tropylium Salts and Aromatic Hydrocarbons

Y. Takahashi, S. Sankararaman, and J. K. Kochi*

Contribution from the Department of Chemistry, University of Houston, University Park, Houston, Texas 77204. *Received September 9, 1988*

Abstract: Tropylium cation ($C_7H_7^+$) forms electron donor–acceptor or EDA complexes with various benzene, naphthalene, and anthracene donors (Ar), as evidenced by the series of brightly colored solutions showing absorption bands that vary with the arene ionization potentials according to Mulliken charge-transfer theory. The spectrophotometric measurement of the formation constants indicates the presence of uniformly weak (1:1) complexes [Ar, $C_7H_7^+$] with $K < 1$ M^{-1} in acetonitrile. However, the successful isolation of single crystals of the unique cationic EDA complex allows X-ray crystallography to establish the charge-transfer (CT) transition as deriving from centrosymmetric layered structures of tropylium–naphthalene pairs at interannular separations of 3.3 Å. The direct correspondence of such solid-state structures with the tropylium EDA complexes in solution is demonstrated by an excellent correlation of the relevant CT energies ($h\nu_{CT}$) obtained from the reflectance and absorption spectra, respectively. Time-resolved spectroscopy following the 532-nm irradiation of the tropylium EDA complex in acetonitrile with a 30-ps laser pulse leads to the resolved picosecond absorption spectra of arene cation radicals within the CT excited (ion-radical pair) state as [$Ar^{\bullet+}$, $C_7H_7^{\bullet}$]. The temporal evolution of the transient $Ar^{\bullet+}$ absorbance with first-order rate constants of $k_1 \geq 4 \times 10^{10}$ s^{-1} for various anthracenes relates to the back-electron-transfer from this ion-radical pair on its return to the original ground-state EDA complex. Such a facile annihilation of the solvent-caged ion-radical pair limits the photochemistry of tropylium EDA complexes to electron donors such as dianthracene and hexamethyl(Dewar benzene) in which the cation radical is highly labile. Thus, the brief lifetime of $Ar^{\bullet+}$ with $\tau \sim 15$ ps largely precludes second-order quenching processes.

Organic cations are electron acceptors by virtue of their electron-deficient centers on one or more carbon atoms.[1] Indeed, the coordinative unsaturation in such stable carbocations as tropylium ($C_7H_7^+$) and triphenylcarbenium (Ph_3C^+) is underscored by their well-known ability to form acid–base complexes with even such weak σ-donors as ethers, nitriles, etc.[2,3] In a similar vein are the intermolecular interactions of tropylium ions with electron-rich anionic donors to form charge-transfer salts that are manifested by the appearance of new absorption bands in the ultraviolet/visible region, both in solution[4,5] and in the crystalline salt.[6] Less obvious are the charge-transfer absorption bands that have been observed between the tropylium[7] or the triphenylcarbenium[8] cation and a series of aromatic π-donors.[7,8] The electron donor–acceptor or EDA interactions in such arene complexes are weak, as shown by the limited magnitude of the formation constant of the 1:1 complex, i.e.

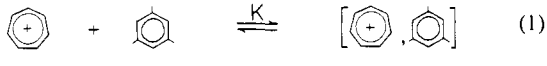

(1)

with $K \simeq 1$ M^{-1} in acetonitrile.[7] These cationic EDA complexes are formally related to the arene dimer cations $(ArH)_2^{\bullet+}$ that are generated from arenes and their cation radicals, e.g.[9,10]

(2)

as well as to the transient precursor complexes in the "hole"-catalyzed cycloadditions of olefinic substrates, e.g.[11]

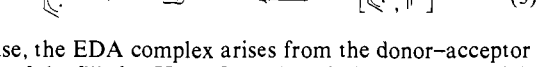

(3)

In each case, the EDA complex arises from the donor–acceptor interaction of the filled π-HOMO on the relatively electron-rich aromatic donor Ar with the unfilled π-LUMO on the electron-deficient cationic acceptor A^+—whether the latter be a persistent diamagnetic cation (eq 1) or a transient paramagnetic cation radical (eq 2 and 3). According to Mulliken,[12] the characteristic new absorption bands result from the charge-transfer excitation ($h\nu_{CT}$) of the weak EDA complex to the radical-ion pair state, i.e.[13]

$$Ar + A^+ \overset{K}{\rightleftharpoons} [Ar, A^+] \xrightarrow{h\nu_{CT}} [Ar^{\bullet+}, A^{\bullet}] \qquad (4a,b)$$

Although the charge-transfer or CT formulation in eq 4 rests on firm theoretical grounds,[14] there exists no direct experimental evidence, crystallographic or spectroscopic, for either the existence of the EDA complex [Ar, A^+] or the formation of the excited ion-radical pair [$Ar^{\bullet+}$, $A^{\bullet}$] from cationic π-acceptors, as given in eq 4.

Since the EDA complexes of carbocations are pertinent to their dynamic behavior generally as reactive intermediates in solution,[15] it is important to delineate the charge-transfer excitation particularly with regard to the nature of the radical-ion pair (eq 4b). Accordingly, in this study we have returned to the EDA complexes

(1) See: Radom, L.; Poppinger, D.; Haddon, R. C. In *Carbonium Ions*; Olah, G. A., Schleyer, P. v. R., Eds.; Wiley: New York, 1976; Vol. 5, pp 2303 ff. Kampar, V. E. *Russ. Chem. Rev.* **1982**, *51*, 107.
(2) Freedman, H. H. *Carbonium Ions* **1973**, *4*, 1501.
(3) Harmon, K. M. *Carbonium Ions* **1973**, *4*, 1579.
(4) (a) Kosower, E. M.; Klinedinst, P. E. *J. Am. Chem. Soc.* **1956**, *78*, 3493. (b) Doering, W. v. E.; Knox, L. H. *J. Am. Chem. Soc.* **1957**, *79*, 352. (c) Kosower, E. M. *J. Am. Chem. Soc.* **1958**, *80*, 3253.
(5) Harmon, K. M.; Cummings, F. E.; Davis, D. A.; Diestler, D. J. *J. Am. Chem. Soc.* **1962**, *84*, 120, 3349.
(6) (a) Kitaigorodski, A. I.; Khotsyanova, T. L.; Struchkov, Ya. T. *Acta Crystallogr.* **1957**, *10*, 797. (b) Bockman, T. M.; Kochi, J. K. *J. Am. Chem. Soc.*, in press.
(7) (a) Feldman, M.; Winstein, S. *J. Am. Chem. Soc.* **1961**, *83*, 3338. (b) Feldman, M.; Graves, B. G. *J. Phys. Chem.* **1966**, *70*, 955.
(8) Dauben, H. J.; Wilson, J. D. *J. Chem. Soc., Chem. Commun.* **1968**, 1629.
(9) Badger, B.; Brocklehurst, B. *Trans. Faraday Soc.* **1969**, *65*, 2582.
(10) Lau, W.; Kochi, J. K. *J. Org. Chem.* **1986**, *51*, 1801.
(11) (a) Bauld, N. L.; Bellville, D. J.; Harirchian, B.; Lorenz, K. T.; Pabon, R. A., Jr.; Reynolds, D. W.; Wirth, D. D.; Chiou, H.-S.; Marsh, B. K. *Acc. Chem. Res.* **1987**, *20*, 371 and references therein. (b) Bauld, N. L. *Tetrahedron*, in press.
(12) (a) Mulliken, R. S. *J. Am. Chem. Soc.* **1952**, *74*, 811. (b) Mulliken, R. S.; Person, W. B. *Molecular Complexes: A Lecture and Reprint Volume*; Wiley: New York, 1969.
(13) Compare: Hilinski, E. F.; Masnovi, J. M.; Kochi, J. K.; Rentzepis, P. M. *J. Am. Chem. Soc.* **1984**, *106*, 8071. For related time-resolved studies of cationic methylviologen EDA complexes with anilines, see: Poulos, A. T.; Kelley, C. K.; Simone, R. *J. Phys. Chem.* **1981**, *85*, 823. Jones, G., II; Malba, V. *Chem. Phys. Lett.* **1985**, *119*, 105.
(14) Hanna, M. W.; Lippert, J. L. In *Molecular Complexes*; Foster, R., Ed.; Crane, Russak: New York, 1973; Vol. 1, p 2 ff.
(15) See: Olah, G. A., Schleyer, P. v. R., Eds. *Carbonium Ions*; Wiley: New York, 1968–76; Vol. I–V.

0002-7863/89/1511-2954$01.50/0

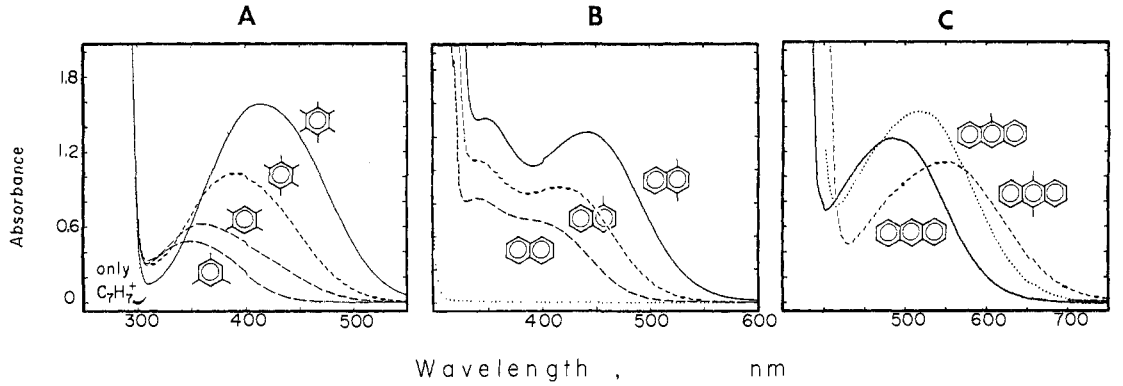

Figure 1. Charge-transfer absorption spectra of tropylium EDA complexes from 2–5 × 10^{-2} M solutions of the various methylated benzene (A), naphthalene (B), and anthracene donors (C) with 1 × 10^{-2} M tropylium tetrafluoroborate in acetonitrile (as indicated). The dotted curve is $C_7H_7^+BF_4^-$ alone at the same concentration.

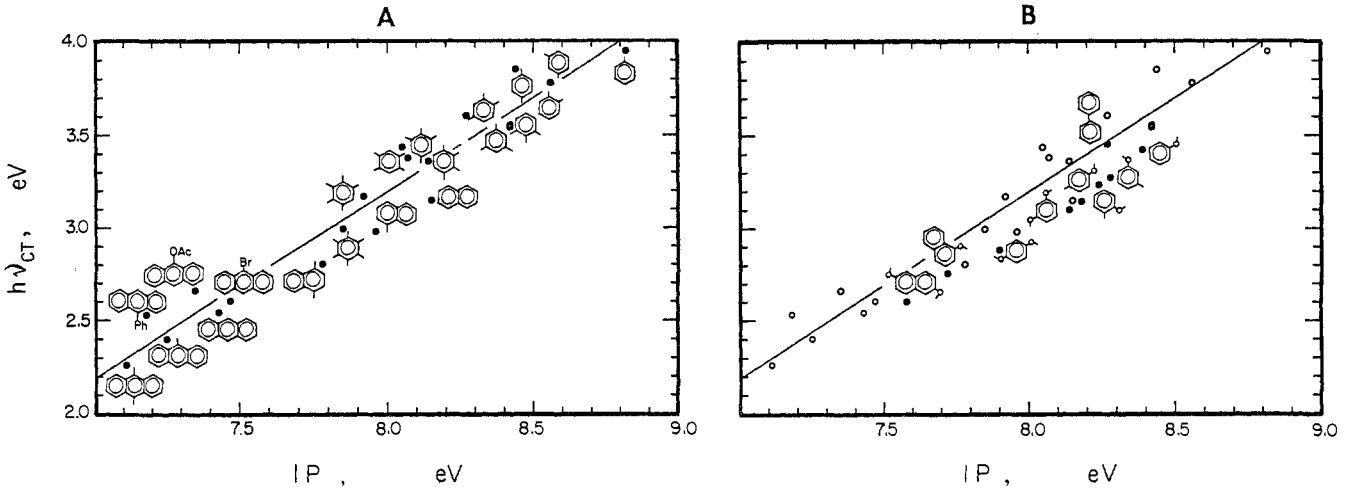

Figure 2. (A) Mulliken correlation of the charge-transfer excitation energies of the tropylium EDA complexes with the ionization potentials of the benzene, naphthalene, and anthracene donors. (b) Inclusion of the methoxyarenes with the same arenes in A.

of the tropylium ion in order (a) to demonstrate the general character of the CT absorption bands with various types of mono- and polynuclear arenes, (b) to measure their formation constants in solution, (c) to isolate single crystals of the EDA complex for the unambiguous X-ray crystallographic determination of their structure, and (d) to establish the radical-ion pair as the reactive intermediate in the CT excitation of the EDA complex by time-resolved picosecond spectroscopy.

Results

Three classes of aromatic hydrocarbons were chosen as representative electron donors: benzenes, naphthalenes, and anthracenes, for their study with the tropylium electron acceptor.

I. Charge-Transfer Spectra of the Tropylium Cationic Acceptor with Various Arene Donors. A colorless solution of tropylium tetrafluoroborate or hexafluoroantimonate in acetonitrile turned pale yellow instantaneously upon exposure to benzene. With naphthalene a bright lemon yellow coloration developed, and a clear red solution resulted from anthracene. The quantitative effects of such dramatic color changes are illustrated in Figure 1 by the appearance of distinctive charge-transfer bands.[9,10] For the series of methylbenzene donors, the absorption maxima λ_{CT} were progressively red-shifted with increasing numbers of methyl substituents (Figure 1A) to reflect the accompanying decrease in the ionization potentials IP (see Table I[16]). A similar bathochromic shift of the charge-transfer band was observed in the tropylium complexes with the series of methylnaphthalenes and methylanthracenes shown in parts B and C of Figure 1, respectively. Such a progressive red shift of the new absorption bands with the ionization potentials of the aromatic donors accords with Mulliken charge-transfer theory.[12] Indeed, for weak EDA complexes, the energy of the charge-transfer transition (i.e. $h\nu_{CT}$) relates directly to the ionization potential by the relationship

$$h\nu_{CT} = IP - E_A - \omega \quad (5)$$

since the electron affinity E_A of the tropylium acceptor is a common value, and the electrostatic work term ω is considered to be constant for related donors.[17] The common CT behavior of the methylbenzenes, naphthalenes, and anthracenes is underscored by the striking linear correlation in Figure 2A, expressed as

$$h\nu_{CT} = 1.0IP - 4.8 \quad (6)$$

with a correlation coefficient of 0.98 to encompass the energy span of almost 2 eV.

The appearance of the clearly resolved second absorption band at higher energies in the naphthalene complexes with tropylium (Figure 1B) was reminiscent of the charge-transfer spectra of other EDA complexes of naphthalene with uncharged acceptors such as tetracyanoethylene, chloranil, tetracyanobenzene, etc.[17,18] The

(16) (a) From: Howell, J. O.; Goncalves, J. M.; Amatore, C.; Klasinc, L.; Wightman, R. M.; Kochi, J. K. *J. Am. Chem. Soc.* **1984**, *106*, 3968. (b) Lau, W.; Kochi, J. K. *J. Am. Chem. Soc.* **1984**, *106*, 7100. (c) Kobayashi, T.; Nagakura, S. *Bull. Chem. Soc. Jpn.* **1974**, *47*, 2563. (d) Watanabe, K.; Nakayama, T.; Mottl, J. *J. Quant. Spectrosc. Radist. Transfer* **1962**, *2*, 369. (e) Clark, P. A.; Brogli, F.; Heilbronner, E. *Helv. Chim. Acta* **1972**, *55*, 1415. (f) Nounou, P. *J. Chem. Phys.* **1966**, *63*, 994. (g) Nagy, O. B.; Dupire, S.; Nagy, J. B. *Tetrahedron* **1975**, *31*, 2453.

(17) Foster, R. F. *Organic Charge-Transfer Complexes*; Academic: New York, 1969.

(18) (a) Andrews, L. J.; Keefer, R. Y. *Molecular Complexes in Organic Chemistry*; Holden-Day: San Francisco, 1964. (b) Briegleb, G. *Elektronen Donator-Acceptor Komplexe*; Springer: Berlin, 1961.

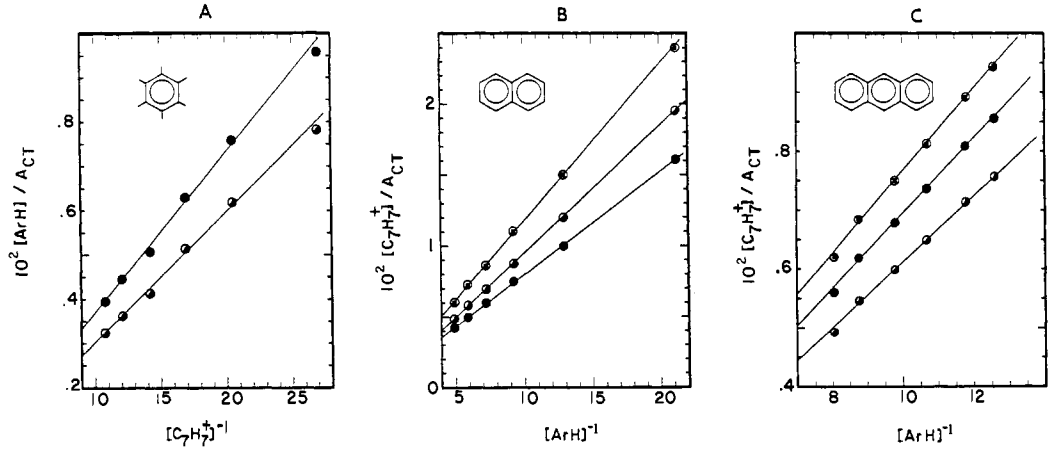

Figure 3. Formation constants of the tropylium EDA complexes by the Benesi–Hildebrand treatment of (A) 3 mM hexamethylbenzene at λ_{mon} = 380 (●) and 415 (◑) nm, (B) 5 mM naphthalene at λ_{mon} = 340 (⊙), 370 (◑), and 420 (●) nm, and (C) 5 mM anthracene at λ_{mon} = 450 (⊙), 488 (●), and 530 (◑) nm in acetonitrile.

Table I. Charge-Transfer Absorption Spectra of Tropylium EDA Complexes and Arene Donors[a]

	IP,[b] eV	λ_{CT},[c] nm	$h\nu_{CT}$, eV
	Methylbenzenes		
benzene	9.23	*d*	
toluene	8.82	~314 (sh)[e]	3.95
1,2-dimethyl	8.56	328	3.78
1,3-dimethyl	8.56	328	3.78
1,4-dimethyl	8.44	322	3.85
1,2,3-trimethyl	8.42	350	3.54
1,2,4-trimethyl	8.27	344	3.60
1,3,5-trimethyl	8.42	349	3.55
1,2,3,4-tetramethyl	8.14	369	3.36
1,2,3,5-tetramethyl	8.07	367	3.38
1,2,4,5-tetramethyl	8.05	361	3.43
pentamethyl	7.92	391	3.17
hexamethyl	7.85	414	2.99
biphenyl	8.27	359 (sh), 313 (sh)	3.45
	Naphthalenes		
naphthalene	8.15, 8.88	393, 341	3.15, 3.63
1-methyl	7.96	416, 341	2.98, 3.63
1,4-dimethyl	7.78	442, 348	2.80, 3.56
1-methoxy	7.72	450, 350 (sh)	2.75, 3.54
2,6-dimethoxy	7.58	476, 375 (sh)	2.60, 3.30
	Anthracenes[f]		
anthracene	7.43, 8.52	488	2.54
9-methyl	7.25	516	2.40
9,10-dimethyl	7.11	548	2.26
9-phenyl	7.18	490	2.53
9-bromo	7.47	476	2.60
9,10-dibromo	7.54	*d*	
9-acetoxy	7.35	466	2.66
9-cyano	7.84	*d*	
9-nitro	7.88	*d*	
	Methoxybenzenes		
anisole	8.39, 9.22	362 (sh), 314 (sh)	3.42, 3.95
1,4-dimethoxy	7.90, 9.12	430, 325 (sh)	2.88, 3.81
1,3-dimethoxy	8.14	400 (sh), 356	3.10
1,2-dimethoxy		410 (sh), 343	3.02
1-methoxy-4-methyl	8.18, 9.11	395, 312 (sh)	3.14, 3.97
1-methoxy-3-methyl	8.28, 8.93	379 (sh), 333	3.27, 3.72
1-methoxy-2-methyl	8.24, 8.93	384 (sh), 331 (sh)	3.23, 3.74

[a] In acetonitrile solution containing 0.01 M $C_7H_7^+BF_4^-$ and 0.05 M Ar unless indicated otherwise. [b] From ref 16 and 50. [c] Absorption maximum, unless indicated otherwise. [d] Unresolved tail absorption. [e] sh = partially resolved shoulder. [f] Contains 0.03 M $C_7H_7^+BF_4^-$ and 0.017 M Ar.

observation of multiple CT transitions in such arene complexes with TCNE has been attributed to electron promotion from different high-lying occupied orbitals of the donor to the lowest unoccupied molecular orbital (LUMO) of the acceptor.[19] This formulation also relates to the observation of multiple CT bands in methoxy-substituted benzenes (Table I, entries 29–35), in which the oxygen lone pairs extend the aromatic conjugation.[20] The unity of these methoxyarenes with their wholly hydrocarbon analogues is illustrated in Figure 2B by the least-squares fit of the new CT data (filled circles) to the same correlation that was established for the hydrocarbons in Figure 2A.[21]

Table II. Formation Constants of Selected Tropylium EDA Complexes with Arene Donors in Solution[a]

arene	λ_{mon},[b] nm	*K*, M^{-1}	ϵ_{CT},[c] M^{-1} cm^{-1}
benzene	320	0.25	1790
toluene	320	0.35	1770
p-xylene	322	0.63	1010
mesitylene	349	0.79	1270
durene	361	0.82	1650
pentamethylbenzene	391	0.86	2560
hexamethylbenzene[d]	414	0.53	6450
anisole	314	0.26	1830
anisole	340	0.44	781
naphthalene	341	0.51	2490
naphthalene	393	0.46	2240
anthracene[d]	488	0.76	2320

[a] In acetonitrile containing ~0.005 M $C_7H_7^+BF_4^-$ and ~0.05 M Ar at 23 °C, unless indicated otherwise. [b] CT wavelength monitored. [c] Extinction coefficient at λ_{mon}. [d] Contains ~0.05 M $C_7H_7^+BF_4^-$ and ~0.004 M Ar.

II. Formation Constants of Tropylium EDA Complexes of Arenes in Acetonitrile Solutions. The thermodynamic stability of the tropylium complexes in solution was ascertained by measuring the formation constants *K* of the three classes of aromatic donors (Ar), i.e.

$$Ar + C_7H_7^+ \overset{K}{\rightleftharpoons} [Ar, C_7H_7^+] \qquad (7)$$

using the spectrophotometric procedure of Benesi and Hildebrand.[22] Owing to the solubility of the tropylium salt $C_7H_7^+BF_4^-$ in acetonitrile, the charge-transfer absorbance A_{CT} was measured with the selected benzene derivatives and naphthalene in excess.

(19) (a) Consistent with this formulation, for the naphthalene EDA complex with tetracyanoethylene, chloranil, and tetracyanobenzene the band gap [$h\nu_{CT}(2) - h\nu_{CT}(1)$] is relatively constant at 0.56, 0.58, and 0.56 eV, respectively. (b) The alternative possibility arising from transitions to several unoccupied orbitals on the tropylium acceptor is not borne out by the gap variation of $\Delta h\nu_{CT}$ = 0.76, 0.71, and 0.56 eV for 1,4-dimethyl-, 1-methyl-, and naphthalene donors.

(20) See: Kaiser, E. T., Kevan, L., Eds. *Radical Ions*; Wiley: New York, 1968. Orchin, M.; Jaffe, H. H. *Symmetry, Orbitals, and Spectra*; Wiley: New York, 1971.

(21) To only the low-energy bands CT_2.

(22) Benesi, H. G.; Hildebrand, J. H. *J. Am. Chem. Soc.* **1949**, *71*, 2703.

Table III. Solid-State CT Absorption Bands of Tropylium EDA Complexes with Arene Donors on Alumina Support[a]

arene	λ_{CT}, nm	$h\nu_{CT}$, eV
hexamethylbenzene	440	2.82
pentamethylbenzene	420	2.95
durene	410	3.02
4-methoxytoluene	400	3.10
1,4-dimethoxybenzene	440	2.82
naphthalene	415	2.98
1,4-dimethylnaphthalene	470	2.64
2,6-dimethoxynaphthalene	500	2.48
anthracene	520	2.38
9-methylanthracene	550	2.25
9,10-dimethylanthracene	570	2.17
9-bromoanthracene	520	2.38
9-phenylanthracene	525	2.36

[a] From 0.5 part each of Ar and $C_7H_7^+BF_4^-$ with 10 parts of alumina (200 mesh) after grinding to fine powder, measured by reflectance against an alumina reference.

Under these conditions the concentration dependence of A_{CT} is given by the Benesi–Hildebrand relationship.[23]

$$\frac{[C_7H_7^+BF_4^-]}{A_{CT}} = \frac{1}{\epsilon_{CT}} + \frac{1}{K\epsilon_{CT}[Ar]} \qquad (8)$$

With the less soluble anthracene derivatives, the tropylium acceptor was employed in excess. Typical Benesi–Hildebrand plots for the formation of the EDA complexes under both of these conditions are illustrated in Figure 3. The linear fit of the absorbance data was obtained by the method of least squares, typically with correlation coefficients $r > 0.99$. The resulting values of the formation constant K and the extinction coefficient ϵ_{CT} at the monitoring wavelength are listed in Table II for some representative arene EDA complexes of the tropylium cation. Among the series of methylbenzenes, there was a slight, but distinct, trend for the formation constants to increase with the number of methyl substituents. Generally, however, the magnitudes of the formation constants were rather limited with $K < 1\ M^{-1}$, as listed in Table II. Accordingly, the tropylium EDA complexes from the benzenes, naphthalene, and anthracenes were all considered to be uniformly weak.

III. Isolation of Tropylium EDA Complexes in the Solid State. Brightly colored solutions of the various anthracenes and tropylium in acetonitrile, either as the tetrafluoroborate, hexafluorophosphate, or hexafluoroarsenate salt, did not deposit the solid EDA complex, even upon cooling until the solvent froze—at which point the mixture merely turned colorless. Phase separation also occurred when cosolvents such as dichloromethane, diethyl ether, or carbon tetrachloride were present, and only the separate components could be isolated. Likewise, the slow evaporation of SO_2 from a bright yellow solution of naphthalene and $C_7H_7^+BF_4^-$, SbF_6^-, or AsF_6^- in liquid sulfur dioxide gradually bleached as the colorless precursors precipitated. An extensive variety of such experiments indicated that the tropylium EDA complexes with arenes were too weak (Table II) to be isolated by crystallization from solution.

We discovered, however, a deposit of bright, yellow crystals when an equimolar mixture of naphthalene and $C_7H_7^+SbF_6^-$ was left in an open tube. The slow evaporation of acetonitrile led to small amounts of EDA crystals only on the walls immediately above the solution–air interface. The same procedure was also effective for the production of orange crystals from mixtures of naphthalene and $C_7H_7^+SbCl_6^-$ or 1,4-dimethylnaphthalene and $C_7H_7^+SbF_6^-$ that were both suitable for single-crystal X-ray crystallography of these tropylium EDA complexes (vide infra). Unfortunately, we were unable to employ the same or modified procedures (despite numerous attempts) to grow crystals of tropylium complexes with any anthracene or benzene donor.

All of the tropylium EDA complexes could be obtained in the solid state, however, by simply grinding equimolar mixtures of the appropriate arene and tropylium salt together with neutral alumina (~100 mesh) to the consistency of a fine colored powder. Thus, the bright yellow solid obtained from naphthalene and $C_7H_7^+BF_4^-$ was visually identical with the charge-transfer color produced from the same donor–acceptor pair in acetonitrile solution (vide supra). For the measurement of the diffuse reflectance spectrum, we found that the solid EDA complexes produced from 1:1 mixtures of tropylium salt and various arenes with 10 parts of the alumina support were optimum for calibration relative to the surface of the neutral alumina reference.[24] It is noteworthy that the same reflectance spectrum was obtained when the preformed crystalline EDA complex (vide supra) was admixed with alumina.[25] In each case the band shape of the powder spectrum was similar to (but slightly broader than) the absorption spectrum obtained in solution,[26] and the absorption maximum in Table III was consistently red-shifted by ~30 nm. Most importantly, the reflectance spectrum of the EDA powder bore a direct relationship to the absorption spectrum of the EDA solution, as shown by the linear correlation in Figure 4. The quantitative relationship of the pair of charge-transfer excitation energies is given by the expression

$$h\nu_{CT}(p) = 0.94h\nu_{CT}(l) + 0.006\ eV \qquad (9)$$

where p and l refer to the EDA powder and solution, respectively.

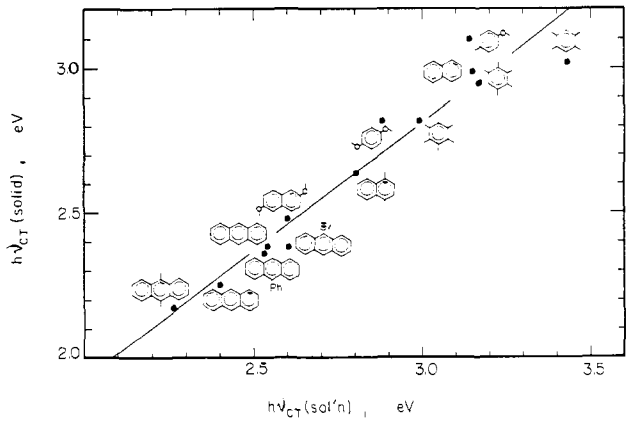

Figure 4. Correlation of the solid-state (reflectance) CT band of the tropylium EDA complex on alumina support with the solution (absorption) CT band of the same complex in acetonitrile.

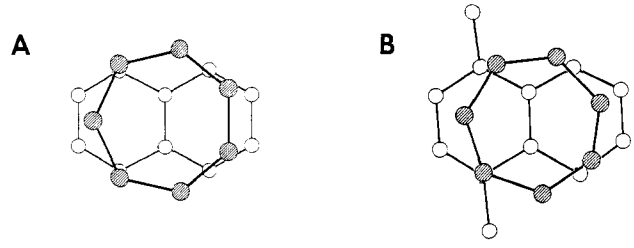

Figure 5. Top projection of the planar (left) tropylium/naphthalene and (right) tropylium/1,4-dimethylnaphthalene pairs extant in the EDA complexes (hexafluoroantimonates) showing the common centrosymmetric structures as discussed in the text.

IV. Molecular Structures of Tropylium EDA Complexes by X-ray Crystallography. The successful isolation of the three colored crystals of the tropylium salts with naphthalene donors (vide supra) allowed X-ray crystallography to establish the origin of the charge-transfer absorptions in these EDA complexes. For example, the X-ray diffraction pattern from the naphthalene complex with $C_7H_7^+SbF_6^-$ obtained as bright yellow orthorhombic

(23) Foster, R. *Molecular Complexes* **1974**, *2*, 107.

(24) Neutral silica but not Celite was also a suitable support (see the Experimental Section).

(25) The substantially higher color intensities obtained from the admixture of the preformed EDA complex indicated that the grinding of the separate components (Ar and $C_7H_7^+BF_4^-$) did not lead to complete EDA formation in the solid mixture.

(26) See: Wright, J. D. *Molecular Crystals*; Cambridge University Press: New York, 1987; p 20 ff.

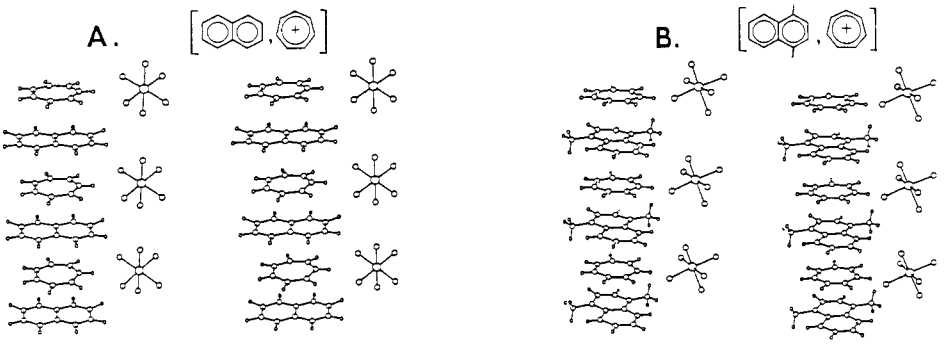

Figure 6. Stereoscopic views of the alternate stacking of (A) naphthalene and tropylium and (B) 1,4-dimethylnaphthalene and tropylium along the *c* axis of the hexafluoroantimonate EDA complexes.

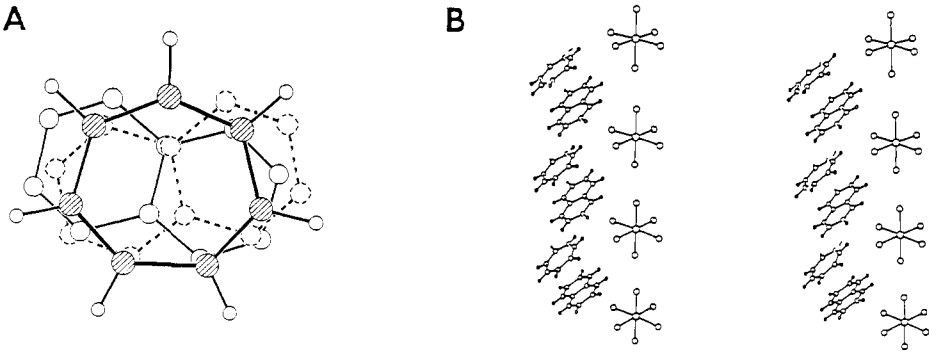

Figure 7. (A) View normal to the tropylium plane showing two disordered naphthalene sites in the $SbCl_6^-$ complex. (B) Stereoscopic view of the naphthalene/tropylium pairs tilted 45° from the stacking axis.

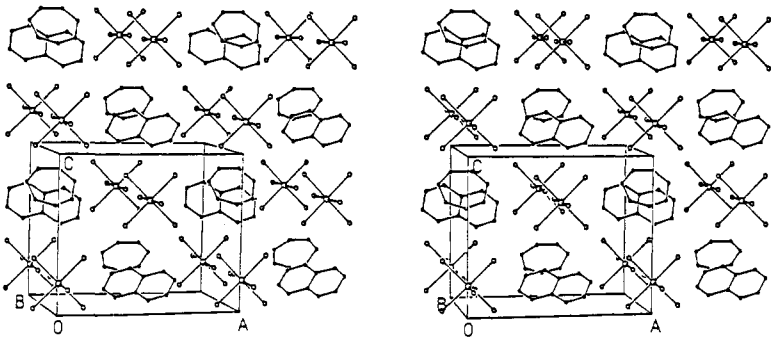

Figure 8. Stereoscopic packing diagram of the unit cell of the naphthalene EDA complex with $C_7H_7^+SbCl_6^-$ clearly delineating the discrete 1:1 donor–acceptor interaction at a separation of 3.34 Å.

crystals was solved (see the Experimental Section) as the 1:1 EDA complex in which the planar tropylium cation was poised centrosymmetrically over the naphthalene nucleus with an interannular separation of 3.36 Å, as illustrated in Figure 5A.

The related unsymmetrical donor 1,4-dimethylnaphthalene with the same tropylium salt $C_7H_7^+SbF_6^-$ afforded orange monoclinic crystals of which the X-ray crystallographic determination established the same basic centrosymmetric structure for the donor–acceptor pair, as shown in Figure 5B. Moreover, the interplanar distance from the tropylium centroid to the naphthalene plane was 3.38 Å despite the presence of two sizable methyl substituents to lower the symmetry of the donor. Otherwise the bond distances and bond angles in the crystalline EDA complexes (see Tables I and II in the supplementary material) were essentially the same as those established earlier for the separate, uncomplexed naphthalene donors and the tropylium salts.[27,28]

The coplanar tropylium–naphthalene pairs are packed in the unit cells of both [$C_{10}H_8$, $C_7H_7^+SbF_6^-$] and [$(CH_3)_2C_{10}H_6$, $C_7H_7^+SbF_6^-$] as a stack of alternating donor–acceptor moieties, with the quasi-spherical counteranion SbF_6^- in a separate column shown in parts A and B of Figure 6. Since the tropylium cation is situated in the stack midway between the overlapping naphthalene nuclei, it was difficult to assign with certainty the discrete structural unit responsible for the relevant charge-transfer transition in the crystal.[29]

The structural situation was much less ambiguous when the larger $SbCl_6^-$ replaced SbF_6^- as the counteranion in EDA crystal. Thus, naphthalene and $C_7H_7^+SbCl_6^-$ afforded orange orthorhombic crystals in which X-ray crystallography located the tropylium centroid atop naphthalene (Figure 7A) at a distance of 3.34 Å, in much the same manner as that shown for the SbF_6^- analogues in Figure 5. However, in this larger unit cell, the tropylium–naphthalene pairs appeared as discrete units owing to

(27) (a) Ahmed, F. R.; Cruickshank, D. W. *Acta Crystallogr.* **1952**, *5*, 852. (b) Cruickshank, D. W. *Acta Crystallogr.* **1957**, *10*, 504.

(28) Previous X-ray crystallographic determinations of tropylium salts were of disordered crystals. (a) Gould, E. S. *Acta Crystallogr.* **1954**, *7*, 113. (b) Kitaigorodshii, A. I.; Khotsyanova, T. L.; Struchkov, Yu. T. *Acta Crystallogr.* **1957**, *10*, 797. (c) Kitaigorodshii, A. I.; Struchkov, Yu. T.; Khotsyanova, T. L.; Volpin, M. E.; Kursanov, D. N. *Izv. Akad. Nauk. SSSR, Ser. Khim.* **1960**, 39.

(29) The contact distance of 3.3 Å was dictated by the dimension of the unit cell owing to the small size of SbF_6^- less than van der Waals distance for contact. This interplanar distance compares with 3.5 Å generally considered for the intermolecular face-to-face separation of aromatic rings. See e.g.: (a) Brock, C. P.; Dunitz, J. D. *Acta Crystallogr.* **1982**, *B38*, 2218. (b) Potenza, J.; Mastropaolo, D. *Acta Crystallogr.* **1975**, *B31*, 2527. (c) Iball, J.; Low, J. N. *Acta Crystallogr.* **1974**, *B30*, 2203.

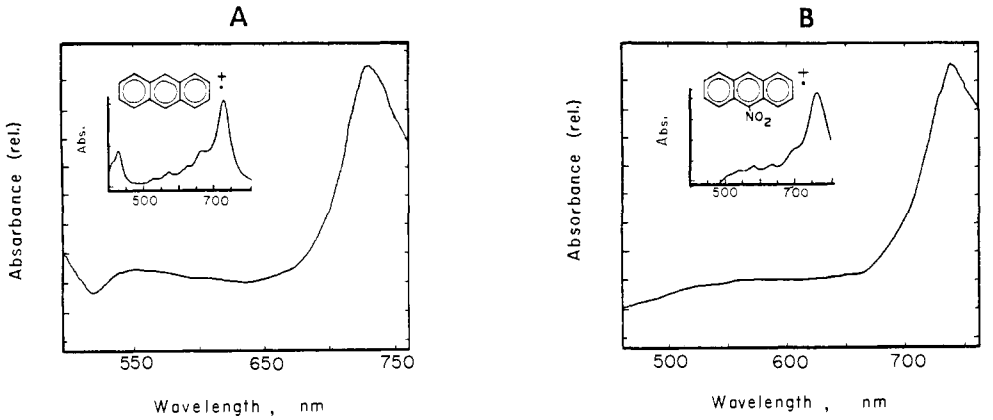

Figure 9. Transient absorption spectrum of the cation radical from (A) anthracene and (B) 9-nitroanthracene at ~35 ps following the 532-nm CT excitation of the tropylium EDA complex in MeCN with the 30-ps (fwhm) laser pulse. The insets are the steady-state spectra obtained by spectroelectrochemical generation of $Ar^{\bullet+}$ in ref 33.

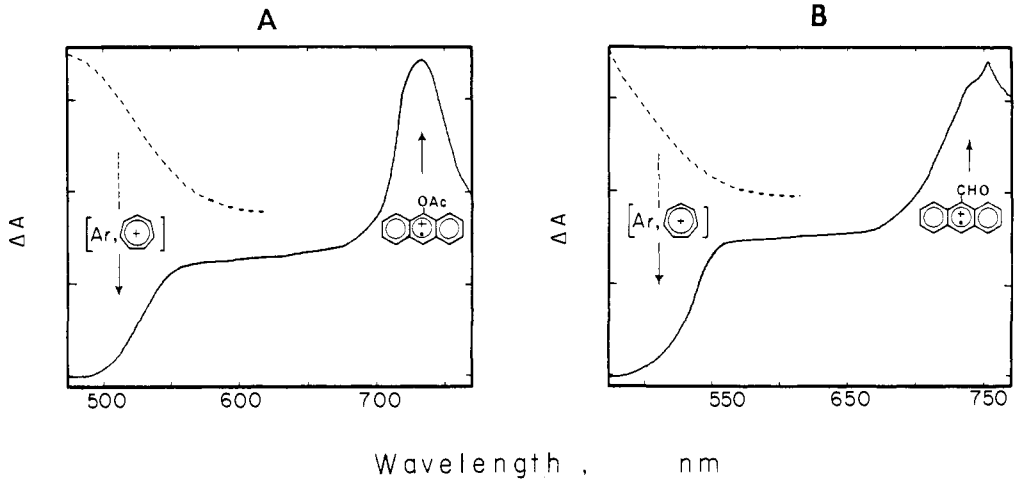

Figure 10. Difference spectra showing the simultaneous growth of the cation radical $Ar^{\bullet+}$ at $\lambda > 700$ nm and the bleaching of the CT band at $\lambda < 550$ nm taken at ~35 ps following the application of the 532-nm laser pulse to the tropylium EDA complex of 9-acetoxyanthracene (A) and 9-anthraldehyde (B) in acetonitrile. For qualitative comparisons, the dashed curves show the low-energy tails of the normal CT spectra (Figure 1 with an arbitrary absorbance scale) prior to irradiation.

an approximately 45° tilt of the tropylium and naphthalene planes from the stacking axis shown in Figure 7B.[30] The discrete electron donor–acceptor interactions leading to the charge-transfer transition with $h\nu_{CT}$ = 415 nm in the crystalline EDA complex is underscored by the stereoscopic view of the unit cell in Figure 8.

V. Observation of the Charge-Transfer Excited State by Time-Resolved Picosecond Spectroscopy of Tropylium EDA Complexes. In order to ascertain the nature of the colored (visible) absorption bands of the tropylium EDA complexes in Figure 1, we examined the time-resolved spectra immediately following the application of a 30-ps pulse consisting of the second harmonic at 532 nm of a mode-locked Nd^{3+}:YAG laser. This wavelength coincided with the maxima of the CT absorption bands of the series of anthracene complexes with the tropylium acceptor in acetonitrile solutions. (See Figure 1C.) Accordingly, the time-resolved spectra obtained from the tropylium–anthracene system related directly to the charge-transfer excitation since there was no ambiguity about the adventitious local excitation of complexed (or uncomplexed) chromophores.[12] Indeed, intense transient absorptions were observed in the visible region between 500 and 750 nm immediately following the CT excitation of the tropylium EDA complexes, as shown in Figure 9. The time-resolved spectra from the anthracene and 9-nitroanthracene donors Ar represented the (normalized) composite of six difference spectra taken in the time interval between 20 and 50 ps after the application of the 532-nm laser pulse.[31] Comparison with the steady-state absorption spectra of the corresponding anthracene cation radicals (see insets) that were independently generated by the spectroelectrochemical technique[32] thus established the identity of the charge-transfer

Table IV. Transient Absorption Spectra of Arene Cation Radicals from the Charge-Transfer Excitation of EDA Complexes[a]

	concn, M	$C_7H_7^+$, M	absorptn max,[b] nm		
			$C_7H_7^+$	TNM[c]	OsO_4[d]
		Anthracene			
anthracene	0.03	0.2	728	710	742
9-methyl	0.02	0.03	700		
9-bromo	0.03	0.06	720	720	720
9-cyano	0.03	0.3	751	770	758
9-nitro	0.05	0.3	746	760	750
9-phenyl	0.03	0.1	735	720	
9-acetoxy	0.05	0.05	735		
9-formyl	0.03	0.2	754	735	
		Naphthalene			
1,4-dimethyl	0.10	0.1	720	720	740

[a] In acetonitrile solution containing Ar and $C_7H_7^+BF_4^-$, as indicated, at 25 °C. [b] For the principal long wavelength band of $Ar^{\bullet+}$ only measured at ~30 ps. [c] From ref 33. [d] From ref 34.

(30) (a) The dimension of the unit cell along the *b* axis was determined by the van der Waals interactions in the columnar stacks of $SbCl_6^-$ units. (b) The tropylium and naphthalene planes are skew ~6° relative to each other.

(31) See the Experimental Section for details.

(32) Hilinski, E. F.; Masnovi, J. M.; Amatore, C.; Kochi, J. K.; Rentzepis, P. M. *J. Am. Chem. Soc.* **1983**, *105*, 6167. See also ref 13.

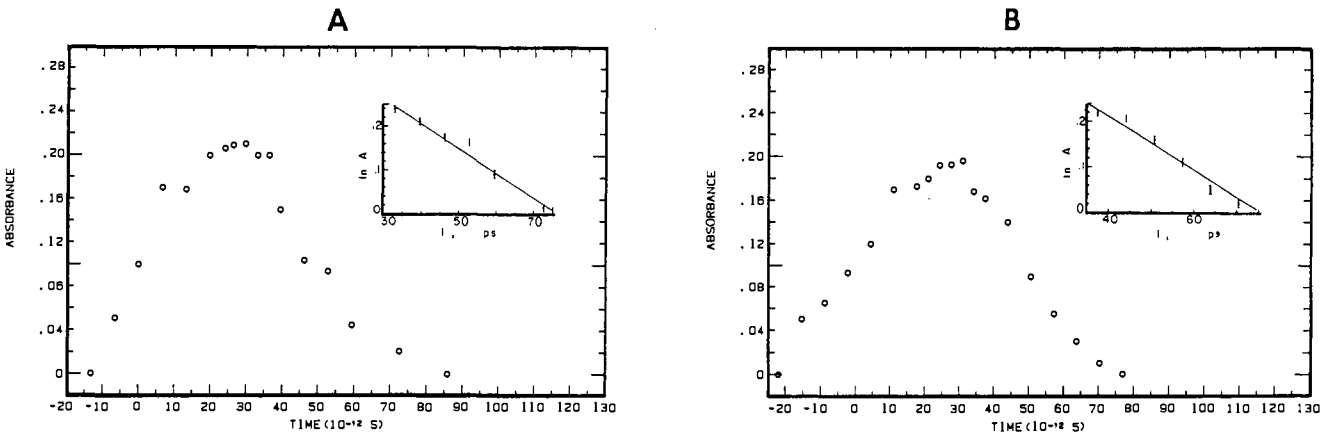

Figure 11. Typical appearance and decay of the CT transients from (A) 9-acetoxyanthracene and (B) 9-anthraldehyde in MeCN by following the absorbance change at λ_{max} = 735 and 754 nm, respectively. The insets show the first-order plots of the absorbance decays subsequent to the maxima at 30–35 ps.

transient. The absorption bands (λ_{max}) of analogous cation radicals $Ar^{\bullet+}$ derived from the CT excitation of the tropylium complexes with other 9-substituted anthracenes are listed in Table IV. Also listed in Table IV for comparison are the principal absorption bands of related $Ar^{\bullet+}$ transients previously produced upon the CT excitation of anthracene EDA complexes with tetranitromethane (column 4)[33] and osmium tetroxide (column 5).[34]

The appearance of the absorption spectra of the anthracene cation radicals in Table IV was accompanied by the disappearance of the charge-transfer absorption bands listed in Table I. The simultaneity of these spectral changes (ΔA) was clearly delineated in those anthracene donors with 9-phenyl, bromo, acetoxy, and formyl substituents owing to the well-defined absorption maxima of their charge-transfer bands (see Table I). Figure 10 typically illustrates the growth of the aromatic cation radicals by the positive absorptions ($\Delta A > 0$) at wavelengths beyond 700 nm concomitant with the depletion of the ground-state EDA complexes by the negative CT absorptions ($\Delta A < 0$) at wavelengths less than 550 nm below the base line.[35] Such a photoinduced disassembling of the ground-state EDA complex readily identified the charge-transfer excitation as

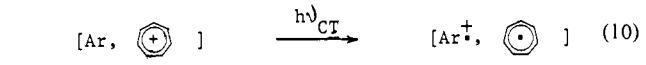

(10)

The accompanying changes in the absorption spectra of the tropyl cation and radical in eq 10 were obscured by their overlap with the dominant absorptions of the aromatic donors below 500 nm.[36]

VI. Charge-Transfer Photochemistry of Tropylium EDA Complexes. Temporal Evolution of Arene Cation Radicals. The transient absorption spectra in Figures 9 and 10 identify $Ar^{\bullet+}$ as the reactive intermediate in the charge-transfer excitation of tropylium EDA complexes according to eq 10. The subsequent disappearance of these cation radicals was followed by measuring the absorbance change at λ_{max} for $Ar^{\bullet+}$ (Table IV) after each laser shot of ~0.16 mJ mm^{-2}. The temporal evolution of the absorbance shown in Figure 11 includes the initial onset for ~20 ps owing the rise time of the 30-ps (fwhm) laser pulse. The first-order plot of the decay portion back to the base line is shown in the inset to the figures.

Table V. First-Order Decay Kinetics of Transient Arene Cation Radicals from the CT Excitation of Tropylium EDA Complexes[a]

	concn, M	$C_7H_7^+$, M	k_1,[b] 10^{-10} s^{-1}	$E°$,[c] V vs SCE	$-\Delta G_{el}$,[d] kcal mol^{-1}
			Anthracene		
anthracene	0.03	0.2	6.6 (3.9)	1.41	36.5
9-methyl	0.02	0.03		1.23	32.5
9-bromo	0.03	0.06	9.0 (3.6)	1.38	35.9
9-cyano	0.03	0.3	6.6 (3.9)	1.74	44.3
9-nitro	0.05	0.3	4.9 (4.5)	1.74	44.3
9-phenyl	0.03	0.1			
9-acetoxy	0.05	0.05	5.7 (4.0)[e]		
9-formyl	0.03	0.2	5.8 (4.0)[f]	1.62	41.5
			Naphthalene		
1,4-dimethyl	0.10	0.1	2.5 (3.8)	1.51[g]	38.8

[a] In acetonitrile solution containing Ar and $C_7H_7^+BF_4^-$ (as indicated) at 25 °C. [b] Values in parentheses corrected for the instrument response function (30 ps) according to $\tau_1^2 = (\tau_m^2 - 30^2)$ where τ_m is the reciprocal of the measured rate constant. See: Rodgers, M. A. J.; Snowden, P. T. *J. Am. Chem. Soc.* **1982**, *104*, 5541. [c] For oxidation of arene, from ref 50. [d] See ref 51b. [e] The first-order rate constant k' measured for the recovery of the ground-state EDA complex at λ = 500 nm is 2×10^{10} s^{-1}. [f] $k_1' = 6 \times 10^{10}$ s^{-1}.

Decay curves similar to those shown in Figure 11 were also observed for the disappearance of the cation radicals from the tropylium EDA complexes with the other anthracenes and naphthalenes. In every case the decay profile followed first-order kinetics. The magnitudes of the first-order rate constant k_1 in Table V were applicable to the complete disappearance of $Ar^{\bullet+}$, as indicated by the return of the cation-radical absorbances back to the base line. The charge-transfer excitation of tropylium EDA complexes from electron-rich arenes such a 9,10-dimethylanthracene and 1-methoxynaphthalene produced transients with very weak absorptions on the picosecond time scale, and reliable spectral and kinetics data could not be obtained.

The photochemical change accompanying the CT excitation was separately monitored by following the absorbance decrease and/or the ^{1}H NMR spectrum of the tropylium EDA complex as it was being subjected to steady-state photolysis. Even after several hours of irradiation with filtered light ($\lambda > 425$ nm) from a 1-kW Hg–Xe lamp, however, the highly colored anthracene complexes failed to undergo any detectable chemical transformation. Similarly, the tropylium EDA complexes of the substituted benzenes and naphthalenes in acetonitrile (Table I) were singularly unchanged after prolonged (6-h) irradiation at $\lambda > 380$ nm.

(33) Masnovi, J. M.; Hilinski, E. F.; Rentzepis, P. M.; Kochi, J. K. *J. Am. Chem. Soc.* **1986**, *108*, 1126.
(34) Wallis, J. M.; Kochi, J. K. *J. Am. Chem. Soc.* **1988**, *110*, 8207.
(35) (a) Note the slight distortion of the negative absorbances arising from the bleaching of the CT band is due to the uncompensated absorptions of $Ar^{\bullet+}$ in this spectral region below ~600 nm. Among the anthracene donors, 9-anthraldehyde and 9-acetoxyanthracene, in Figure 10, are the least affected (e.g., compare with the other analogues in Figure 9). (b) Interference from the ground-state EDA complexes is negligible in the spectral region 650–800 nm where the principle bands of various $Ar^{\bullet+}$ lie. Since the true absorbances of $Ar^{\bullet+}$ transients in this region are thus minimally affected by the CT bleaching, Figures 9 and 10 are based on the direct measurement of the relative absorbance rather than the less direct absolute absorbances of corrected spectra.
(36) (a) These time-resolved spectral studies are regretably limited to the region between 400 and 800 nm, as dictated by the white light continuum of the probe (see the Experimental Section). (b) For the tropylium cation, λ_{max} = 275 nm (ϵ = 4400 M^{-1} cm^{-1}).[4b] (c) For the tropyl radical, λ_{max} = 315 nm (ϵ = 2800 M^{-1} cm^{-1}): Schöneshöfer, M. *Z. Naturforsch.* **1971**, *B26*, 1120.

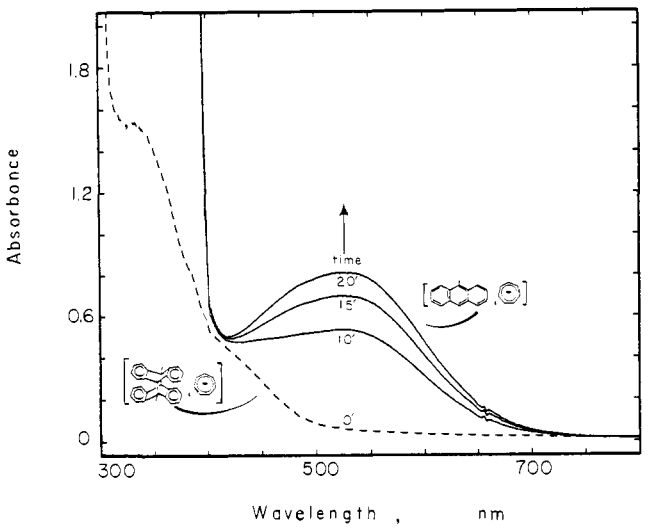

Figure 12. Charge-transfer cycloreversion of 3.3 mM 9-methylanthracene dimer $(MeAn)_2$ with 0.15 M $C_7H_7^+BF_4^-$ (---) in 1:1 CH_2Cl_2/MeCN at 23 °C by following the growth of the CT band of [MeAn, $C_7H_7^+$] with λ_{CT} = 525 nm (—) upon the constant irradiation [$\lambda > 380$ nm for 10, 15, and 20 min (bottom to top)].

Dianthracene (as the head-to-tail 9,10-dimer) is optically transparent above 300 nm owing to the presence of only benzenoid chromophores.[37] Accordingly, the solution of tropylium salt admixed with dianthracene in acetonitrile afforded the yellow CT color showing the characteristic absorption band at 340 nm of the EDA complexes with benzenoid donors (compare Figure 1A).[38] The irradiation of this solution at $\lambda > 380$ nm using a sharp cutoff filter differed dramatically from that observed with the methylbenzene donors (vide supra). Thus, the pale yellow solution rapidly turned deep purple within 10 min, and inspection of the absorption spectrum clearly revealed the growth of a new band with λ_{max} = 490 nm. The series of accompanying color changes are illustrated in Figure 12 for the 9-methyl analogue owing to its slightly better solubility properties. The new absorption band with λ_{max} = 525 nm (Figure 1C) was readily assigned to the tropylium EDA complex of the monomeric donor 9-methylanthracene, i.e.

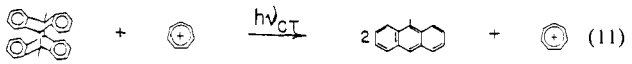

(11)

Since this fragmentation arose directly via the photoexcitation of the EDA complex of dianthracene with tropylium cation, it is designated as *charge-transfer cycloreversion*.[38] The quantum yield of Φ_p = 0.02 for the CT cycloreversion in eq 11 was measured with Reinecke actinometry[39] by the spectrophotometric analysis of 9-methylanthracene (see the Experimental Section).

The charge-transfer cycloreversion of the dianthracene in eq 11 has an intramolecular analogue in the CT isomerization of hexamethyl(Dewar benzene) or HMDB. For example, when HMDB in acetonitrile was exposed to tropylium salt at −30 °C,[40] the solution turned yellow immediately and the CT absorption band of the tropylium EDA complex was readily discerned with λ_{max} = 375 nm. Exposure of this solution to actinic radiation with $\lambda > 380$ nm (using a sharp cutoff filter with a 500-W high-pressure Hg lamp) resulted in the rapid intensification of the color and change to an orange solution (Figure 13). The difference absorption spectrum after 15 min of irradiation revealed a well-resolved absorption band with λ_{max} = 414 nm (see inset) that was

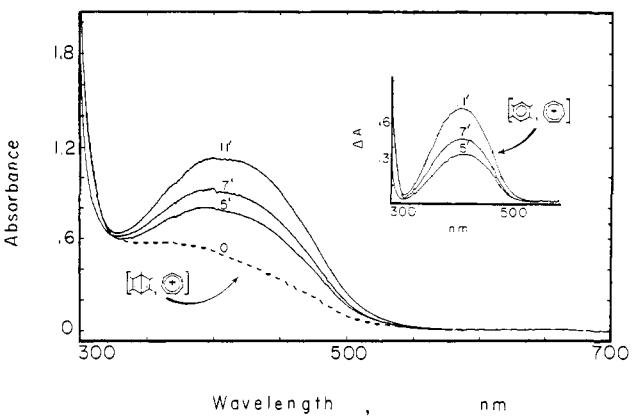

Figure 13. Charge-transfer isomerization of 0.05 M hexamethyl(Dewar benzene) with 0.05 M $C_7H_7^+BF_4^-$ (---) in MeCN at −30 °C by following the growth of the CT band of hexamethylbenzene EDA complex for 5, 7, and 11 min upon irradiation as in Figure 12. The inset identifies the difference CT spectrum as that of [HMB, $C_7H_7^+$].

identical with the charge-transfer spectrum of the tropylium EDA complex with hexamethylbenzene in Figure 1A, i.e.[41]

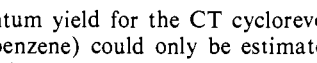

(12)

The quantum yield for the CT cycloreversion of hexamethyl(Dewar benzene) could only be estimated by the absorbance change of the charge-transfer band of the tropylium EDA complex of hexamethylbenzene (see the Experimental Section).

Discussion

Colored solutions of the tropylium cation obtained immediately upon exposure to various benzenes, naphthalenes, and anthracenes (Figure 1) show the typical earmarks of charge-transfer absorption bands, the Mulliken energy $h\nu_{CT}$ varying linearly with the ionization potentials of all the aromatic donors over a span of 50 kcal mol^{-1} with unit slope (eq 6) for the correlation in Figure 2. Such an extensive relationship derives from the 1:1 complexes that are formed according to eq 7 from the tropylium cation in solution with each of the aromatic donors (Ar). Furthermore, the same (or closely related) complexes are produced in alumina and silica matrices, as established by the correlation in eq 9 for the charge-transfer transitions that are applicable even in the solid state.[42,43] The relative ease of formation of all such tropylium EDA complexes, however, belies their isolation uniformly as crystalline structures amenable to X-ray crystallographic determination. Thus, with the appropriate experimental control of neutral arene donors with the cationic tropylium acceptor, we can prepare single crystals of only the naphthalene EDA complexes. We believe that our inability to isolate the analogous benzene and anthracene complexes (despite an increased understanding of the requisite factors for the growth of these mixed-charge complexes)[44] indicates a substantially diminished energy in the crystalline lattice that is not revealed by the magnitudes of the formation constant K in solution (see Table II). It is important to emphasize that the X-ray crystal structures in Figures 5–7 establish the critical interannular separation of 3.3 ± 0.1 Å for the charge-transfer interaction in the tropylium EDA complexes.

It is also singularly noteworthy that the molecular structures of the naphthalene EDA complexes in Figures 5–7 all share in

(37) Bouas-Laurent, H.; Castellan, A.; Desvergne, J. P. *Pure Appl. Chem.* **1980**, *52*, 2633.
(38) Masnovi, J. M.; Kochi, J. K. *J. Am. Chem. Soc.* **1985**, *107*, 6781.
(39) Wegner, E. E.; Adamson, A. W. *J. Am. Chem. Soc.* **1966**, *88*, 394.
(40) At this temperature, the competition from the thermal isomerization of HMDB catalyzed by tropylium cation was insignificant (see the Experimental Section).
(41) Since the time-resolved spectroscopy of an acetonitrile solution of 0.1 M hexamethylbenzene and 0.2 M tropylium tetrafluoroborate upon excitation at 532 nm showed no transient signal for the hexamethylbenzene cation radical (λ_{max} = 490 nm),[56] we tentatively conclude that its lifetime is <10 ps.
(42) See: Herbstein, F. H. In *Perspectives in Structural Chemistry*; Dunitz, J. D., Ibers, J. A., Eds.; Wiley: New York, 1971; Vol. 4, p 166 ff. Prout, C. K.; Kamenar, B. *Mol. Complexes* **1973**, *1*, 152.
(43) Soos, Z. G.; Klein, D. J. *Mol. Assoc.* **1975**, *1*, 2.
(44) Experimentally the difficulty lies in the selective crystallization of the weak tropylium EDA complex in the teeth of the preferential crystallization of the ionic salt ($C_7H_7^+X^-$) and/or the neutral arene (Ar) separately.

common the centrosymmetric location of the tropylium acceptor over the C_{10} naphthalene nucleus, despite either an unsymmetric placement of a pair of methyl substituents (as in Figure 5B for 1,4-dimethylnaphthalene) or a substantial increase in the unit cell dimensions (by the larger $SbCl_6^-$ in Figure 7B). We thus conclude that the centrosymmetric structure of the complex is inherent to the donor–acceptor interaction between naphthalene and tropylium at a separation of 3.3 Å. Indeed the pair of absorption bands illustrated in Figure 1B can be accounted for by the charge-transfer transitions from the highest occupied molecular orbital (HOMO) and subjacent HOMO-1 depicted below.[45,46]

As such, the centrosymmetric structures in Figures 5 and 7A accord with the optimum overlap of the naphthalene HOMO and HOMO-1 of a_u and b_{1u} symmetry, respectively, with the degenerate pair of tropylium e_2'' LUMOs of the same gross symmetry, i.e.

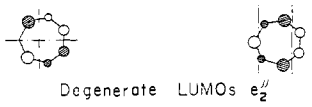

On the basis of similar considerations of orbital symmetry, the EDA complexes of tropylium with neither benzene nor anthracene donors would be centrosymmetric.[47] Be that as it may, the revelant charge-transfer transitions for the EDA complexes in solution do not appear to differ according to the symmetry of the donor–acceptor interactions (e.g., various η^2 and η^6 benzene complexes[48]).

The time-resolved spectroscopic observation of $Ar^{\bullet+}$ accompanying the excitation of the charge-transfer band of the EDA complex accords with the electron promotion from the filled HOMO (or HOMO-1) of the arene donor Ar to the empty LUMO of the tropylium acceptor. Parts A and B of Figure 11 identify the formation of arene cation radicals to occur within the rise time of the 30-ps laser pulse. (The accompanying presence of the tropyl radical is obscured by the arene absorptions.[36]) We conclude that the electron transfer from the arene donor to the tropylium acceptor in the EDA complex effectively occurs with the absorption of the excitation photon ($h\nu_{CT}$) in accord with Mulliken's theory.[12,13] Therefore, our studies establish the sequence of chemical steps in the charge-transfer excitation of the tropylium acceptor and the arene donor as

Scheme I

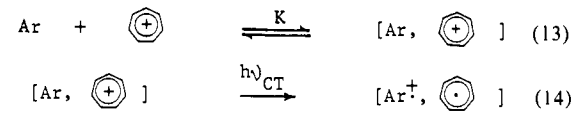

In the absence of any discernible charge-transfer photochemistry (vide supra), the subsequent decay of the cation-radical absorbance in Figure 11 derives from a dark (adiabatic) process. The latter is readily identified as back-electron-transfer since the half-life for the $Ar^{\bullet+}$ decay of $\tau = 17$ ps is essentially the same as the half-life for the recovery of the CT band of the EDA complex (see Table V under 9-anthraldehyde and 9-acetoxyanthracene). Since the observed first-order rate constants k_1 in Table V are too fast to allow significant competition from diffusive separation,[49] the annihilation of $Ar^{\bullet+}$ is ascribed to the reversal of the solvent-caged pair in eq 14 to regenerate the EDA complex, i.e.

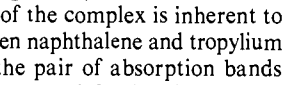

The magnitudes of the driving force $-\Delta G_{et}$ for the back-electron-transfer in eq 15 were evaluated in Table V (column 6) from the redox potentials $E°$ of the anthracenes and tropylium cation.[50,51] In every case the driving force for the return of $Ar^{\bullet+}$ to the arene EDA complex is overwhelmingly large, with $k_1 \geq 4 \times 10^{10}$ s^{-1}.[52]

The rapidity of the back-electron-transfer in eq 11 underlies the singular absence of productive photochemistry accompanying the continuous irradiation of the tropylium EDA complexes of various anthracene, naphthalene, and benzene donors. Accordingly, the photostationary state during charge-transfer excitation is schematically depicted as

Scheme II

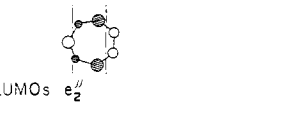

According to this formulation any photochemical transformation resulting from the CT excitation of the tropylium EDA complex is limited by the $Ar^{\bullet+}$ lifetime of $\tau \sim 15$ ps in Table V. Although these inextensible lifetimes discourage competition from any process involving the diffusive separation of the radical pair formed in eq 14,[13] the kinetics obstacle can be circumvented by a *unimolecular* process involving either the arene ion radical, the tropyl radical, or both in the solvent cage. Let us first consider the unimolecular fragmentation and rearrangement of $Ar^{\bullet+}$ as follows.

A. The cycloreversion of the dianthracene An_2 in eq 11 is a direct consequence of populating the charge-transfer excited state of the tropylium EDA complex.[53] The photoefficiency of this charge-transfer cycloreversion is thus limited by the unimolecular rate of fragmentation (k_f) of the dianthracene cation radical relative to back-electron-transfer, i.e.

Scheme III

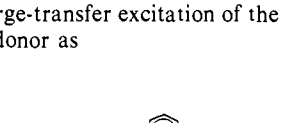

The measured quantum yield of $\Phi_p = 0.02$ for the CT cycloreversion indicates that the rate constant k_{el} for back-electron-transfer in Scheme III (eq 18) is $\sim 10^{10}$ s^{-1} since the half-life of

(45) Salem, L. *Molecular Orbital Theory of Conjugated Systems*; Benjamin: New York, 1966.

(46) Heilbronner, E.; Bock, H. *Das HMO-Modell und Seine Anwedung*; Verlag Chemie: Weinheim, FRG, 1970.

(47) For example, in benzene the degenerate E_{1g} HOMOs predict an unsymmetric EDA complex. Complexation to anthracene in the A/B rings[46] will be analogous to that in naphthalene. It is noteworthy that the naphthalene π dimer cation is also centrosymmetric and related to the structures in Figure 5. See: Fritz, H. P.; Gebauer, H.; Friederich, P.; Ecker, P.; Artes, R.; Schubert, U. *Z. Naturforsch.* **1978**, *33B*, 498.

(48) Compare the benzene EDA complexes of $Hg(O_2CCF_3)_2$ in ref 10 and of halogen: Hassell, O.; Stromme, K. O. *Acta Crystallogr.* **1958**, *12*, 1146; **1958**, *13*, 1781).

(49) Compare: Masnovi, J. M.; Kochi, J. K. *J. Am. Chem. Soc.* **1985**, *107*, 7880.

(50) For the anthracenes, $E_{ox}°$ in Table V from: Masnovi, J. M.; Seddon, E. A.; Kochi, J. K. *Can. J. Chem.* **1984**, *62*, 2552.

(51) (a) For tropylium cation, $E_{red}° = -0.18$ V vs SCE in MeCN from: Wasielweski, M. R.; Breslow, R. *J. Am. Chem. Soc.* **1976**, *98*, 4222. (b) The driving force was taken as $-\Delta G_{et} = \Delta E° = E_{ox}° + E_{red}°$ by neglecting the radical pair interactions in [Ar$^{\bullet+}$, $C_7H_7^{\bullet}$].

(52) (a) The more or less constant values of the rate constants in Table V after correction for the instrument response function could indicate that k_1 is actually $>4 \times 10^{10}$ s^{-1}. (b) Alternatively, the relatively constant rate of back-electron-transfer (despite large differences in ΔG_{et}) is readily understandable if cognizance is taken of the limiting value of the Brønsted slope $\beta = 0$ of the free energy relationship for electron transfer at the exergonic limit of the driving force as described by: Klingler, R. J.; Kochi, J. K. *J. Am. Chem. Soc.* **1982**, *104*, 4186.

(53) Owing to the limited solubility of the dianthracenes, we could not achieve sufficient CT absorbances (>1.5) for the time-resolved spectroscopic studies similar to those in Table IV. This deficiency will be hopefully remedied by the synthesis of more soluble analogues.

Table VI. X-ray Data Collection and Process Parameters for the Tropylium EDA Complexes

	$[Me_2C_{10}H_6, C_7H_7^+SbF_6^-]$	$[C_{10}H_8, C_7H_7^+SbCl_6^-]$	$[C_{10}H_8, C_7H_7^+SbF_6^-]$
space gp	$P2_1$, monoclinic	$Pmn2_1$, orthorhombic	$Pmmn$, orthorhombic
cell constants			
a, Å	6.773 (2)	12.352 (3)	11.186 (4)
b, Å	17.236 (7)	8.044 (2)	11.761 (3)
c, Å	8.348 (2)	10.695 (3)	6.840 (2)
β, deg	101.24 (2)		
V, Å^3	956	1063	900
formula wt	483.13	553.77	455.07
formula units per cell (Z)	2	2	2
density (ρ), g cm^{-3}	1.68	1.73	1.68
absorptn coeff (μ), cm^{-1}	15.0	20.7	15.9
collctn range	$4° \leq 2\theta \leq 55°$	$4° \leq 2\theta \leq 50°$	$4° \leq 2\theta \leq 55°$
scan width $\Delta\theta$, deg	$1.45 + (K\alpha_2 - K\alpha_1)$	$1.50 + (K\alpha_2 - K\alpha_1)$	$1.4 + (K\alpha_2 - K\alpha_1)$
scan speed range, deg min^{-1}	3.0–15.0	1.5–15.0	1.5–15.0
total data collctd	2260	1040	1139
independent data, $I > 3\sigma(I)$	1423	851	619
$R = \sum\|\|F_o\| - \|F_c\|\|/\sum\|F_o\|$	0.027	0.039	0.056
$R_w = [\sum w(\|F_o\| - \|F_c\|)^2/\sum w\|F_o\|^2]^{1/2}$	0.027	0.038	0.038
weights (w)	1.0	$\sigma(F)^{-2}$	$\sigma(F)^{-2}$

the dianthracene cation radical $An_2^{\bullet+}$ was previously estimated to be $\sim 10^{-8}$ s.[38] Indeed the magnitude of k_{et} for the back-electron-transfer in eq 18 evaluated by this indirect method is comparable to the values of k_1 in Table V obtained directly from the first-order decay of the arene cation radical.

B. The isomerization of hexamethyl(Dewar benzene) HMDB in eq 12, like that of the dianthracene (vide supra), occurs as a direct consequence of the actinic activation of the tropylium EDA complex. Accordingly, the charge-transfer mechanism for the aromatization of HMDB can be analogously presented as

Scheme IV

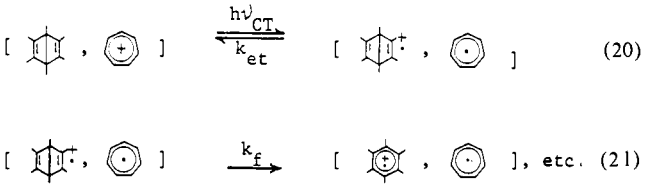

The quantitative examination of the CT isomerization as presented in Scheme IV was unfortunately beset by complications arising from the severe competition from a thermal process.[54] Although the rate of the catalytic isomerization of HMDB by the tropylium cation was retarded at −30 °C, sufficient to establish the occurrence of the CT isomerization (see the Experimental Section), it precluded a definitive examination of the time-resolved spectrum of the CT transient from HMDB in eq 20, as well as a reliable measurement of the quantum yield for eq 12. Nonetheless, the preliminary evaluation of $\Phi_p \sim 4$ suggests the participation of a chain process similar to the HMDB isomerization that Jones, Schuster, and co-workers reported earlier with other electron acceptors by both excited-state quenching and CT activation.[56] If so, an additional pathway involving the cation-radical chain process of the type proposed earlier[57] must be included in Scheme IV. Although our delimiting experiments with HMBD shed little additional light that is not elucidated in the elegant studies of Jones, Schuster, and co-workers,[56,58] they do raise the question as to which cation radical escapes back-electron-transfer in Scheme IV to a degree dictated by second-order kinetics for the chain propagation. Thus, our other photochemical studies directed at the interception of such CT cation radicals by second-order processes have been unfruitful. For example, arene cation radicals are known to readily undergo both nucleophilic addition as well as deprotonation of methyl substituents.[59] In particular, the cation radicals of 9-methyl- and 9,10-dimethylanthracene are particularly stable, and they persist in the time-resolved studies of the CT excitation of the corresponding tropylium EDA complexes for rather prolonged times (vide supra). Our attempts to intercept these methylarene cation radicals in the presence of added bases such as the hindered 2,6-di-*tert*-butylpyridine and 2,4,6-collidine led to no change of the transient behavior, and the parent methylarenes were recovered intact even after prolonged CT irradiation (see the Experimental Section). The more reactive cation radicals from hexamethylbenzene and 1,4-dimethylnaphthalene upon similar exposure yielded no charge-transfer photochemistry and yielded neither products of nuclear addition nor side-chain deprotonation. Further attempts to intercept the transient anthracene cation radical formed by the charge-transfer excitation of the tropylium EDA complex in either acetic acid or methanol solution led to no discernible photochemistry.

Such trapping studies thus confirm the results in Table VI arising from the direct observation of the CT transients by time-resolved picosecond spectroscopy. In order for effective CT photochemistry of arenes to occur via tropylium EDA complexes, a unimolecular process is required to effectively compete with $Ar^{\bullet+}$ lifetimes of ~ 15 ps. The latter largely precludes bimolecular quenching by second-order kinetics, except in those unusual cases such as the HMDB aromatization, in which leakage from the cage[60] can be highly magnified by a subsequent chain process.

Experimental Section

Materials. Benzene (Mallinkrodt), toluene (Eastman), *o*-, *m*-, and *p*-xylene (Aldrich), mesitylene (Baker), 1,2,3-trimethylbenzene (Aldrich), and 1,2,4-trimethylbenzene (Aldrich), all of reagent grade, were repurified by distillation. Durene (Aldrich), pentamethylbenzene (Aldrich), and hexamethylbenzene (Fluka) were recrystallized from ethanol. Naphthalene (Allied Chemical), 1-methylnaphthalene (Aldrich), 1-

(54) Under the reaction conditions of CT isomerization of HMDB (vide supra), the thermal catalysis by tropylium cation was half complete in ~8 h in the dark. The thermal isomerization was accompanied by the growth of a new absorption band at λ_{max} = 474 nm (as yet unidentified) that was gradually overwhelmed by the CT band of HMB as the isomerization progressed.

(55) For the relevant cation radicals in this system, see: (a) Rhodes, C. J. *J. Am. Chem. Soc.* **1988**, *110*, 4446. (b) Roth, H. D.; Schilling, M. L. M.; Raghavachari, K. *J. Am. Chem. Soc.* **1984**, *106*, 253 and references therein.

(56) (a) Jones, G., II; Becker, W. G. *J. Am. Chem. Soc.* **1983**, *105*, 1276. (b) Peacock, N. J.; Schuster, G. B. *J. Am. Chem. Soc.* **1983**, *105*, 3632.

(57) Evans, T. R.; Wake, R. W.; Sifain, M. M. *Tetrahedron Lett.* **1973**, 701.

(58) Solvent polarity studies of fluorescence to probe the cage rearrangement of HMBD to HMB has been suggested by a reviewer (compare ref 56a).

(59) For a recent review, see: Yoshida, K. *Electrooxidation in Organic Chemistry*; Wiley: New York, 1984; p 156 ff.

(60) Factors involved in the cage escape are not as yet completely delineated. For example, the lifetimes of $An_2^{\bullet+}$ and $HMDB^{\bullet+}$ in Schemes III and IV were assumed to be independent of the caged (acceptor) partner, be it $C_7H_7^{\bullet}$, $TCNE^{\bullet-}$, $FUM^{\bullet-}$, etc.,[56,57] despite the different exergonicities ($h\nu_{CT} - \Delta E°$) for radical pair formation. Note with dianthracene and hexamethyl(Dewar benzene) an additional value of the cycloreversion and isomerization energies of 36 and 60 kcal mol^{-1}, respectively.[61,62]

(61) Greene, F. D. *Bull. Soc. Chim. Fr.* **1960**, 1356.

(62) (a) Oth, J. F. M. *Angew. Chem., Int. Ed. Engl.* **1968**, *7*, 646. (b) Adam, W.; Chang, J. C. *Int. J. Chem. Kinet.* **1969**, *1*, 487.

methoxynaphthalene (Aldrich), and 1,4-dimethylnaphthalene (Aldrich) were used as received. 2,6-Dimethoxynaphthalene (Aldrich) was recrystallized from a mixture of dichloromethane and hexane. Anthracene (Aldrich, gold label), 9,10-dimethylanthracene, 9-anthraldehyde, and 9-acetoxyanthracene (Aldrich) were used as received. The following anthracene derivatives (Aldrich) were recrystallized from the solvents: 9-methyl (methanol), 9-cyano (ethanol), and 9-nitro (ethanol–water). The dimers of anthracene and 9-methylanthracene were synthesized by previously reported procedures.[38] Hexamethyl(Dewar benzene) (Aldrich) was purified by distillation in vacuo and stored at −20 °C in the dark. Tropylium tetrafluoroborate was prepared from tropylidene (Shell) according to the literature procedure[63] and recrystallized from an acetonitrile/ethyl acetate mixture. ^{1}H NMR (CD_3CN): 9.30 (s) ppm. IR (KBr): 2991 (w), 1636 (w), 1477 (s), 1078 (s, BF_4^-), 1031 (s), 660 (m) cm^{-1}. Tropylium tetrafluoroarsenate, tropylium hexafluoroantimonate, and tropylium hexachloroantimonate were prepared as follows.[64] Cycloheptatriene (0.6 mL, 5.8 mmol) was added to a stirred red-orange solution of triphenylmethyl hexafluoroantimonate (2.4 g, 5 mmol) in acetonitrile (7 mL) under an argon atmosphere. Upon stirring for 15 min, the solution turned pale yellow. Anhydrous ether (50 mL) was added, and the precipitated tropylium hexafluoroantimonate was removed by filtration and washed several times with ether. It was recrystallized from a mixture of acetonitrile and ethyl acetate at −20 °C. The yield of tropylium hexafluoroantimonate was 68%. ^{1}H NMR (CD_3CN): 9.24 (s) ppm. IR (KBr): 3032 (s), 1480 (s), 993 (w), 654 (s, SbF_6^-) cm^{-1}. Tropylium hexafluoroarsenate was prepared from cycloheptatriene (0.25 mL, 2.4 mmol) and triphenylmethyl hexafluoroarsenate (1.0 g, 2.3 mmol) as described above; yield 62%. ^{1}H NMR (CD_3CN): 9.23 (s) ppm. IR (KBr): 3033 (s), 1483 (s), 993 (w), 703 (s, AsF_6^-), 665 (m), 641 (s) cm^{-1}. For tropylium hexachloroantimonate, a mixture of triphenylmethyl chloride (2.78 g, 10 mmol) and antimony pentachloride (3.0 g, 10 mmol) was stirred in acetonitrile (25 mL) for 15 min under argon. Cycloheptatriene (1.2 mL, 12 mmol) was added to the mixture, and stirring was continued for additional 15 min. The reaction mixture was worked up as described above to yield tropylium hexachloroantimonate as a pale yellow solid, yield 70%. ^{1}H NMR (CD_3CN): 9.30 (s) ppm. Ir (KBr): 3000 (w), 1470 (s), 1285 (w), 655 (m), 630 (s), 330 (s, $SbCl_6^-$) cm^{-1}. Triphenylmethyl hexafluoroarsenate and hexafluoroantimonate (Ozark–Mahoning) were used as received. Acetonitrile (Fisher) and dichloromethane (Fisher) were distilled from P_2O_5 and stored under an argon atmosphere. Ether (Baker) was distilled from lithium aluminum hydride and stored under an argon atmosphere. Ethyl acetate (Fisher, HPLC grade) was used without further purification.

Instrumentation. The electronic spectra were recorded on a Hewlett-Packard 8450A diode-array UV–vis spectrometer. The diffuse reflectance spectra of the solid samples were measured on a Perkin-Elmer 330 UV–vis spectrometer, equipped with a Hitachi 210-2101 integrating sphere. An alumina disk was used as the reference for the diffuse reflectance spectral measurements. NMR spectra were recorded on a JEOL FX 90Q spectrometer (90 MHz). Proton chemical shifts are reported in ppm downfield from the $(CH_3)_4Si$ internal standard. IR spectra were recorded on a Nicolet 10DX FT spectrometer. GC analyses were carried out on a Hewlett-Packard 5790A chromatograph using a 12.5-m SE-30 (cross-linked methylsilicone) capillary column. The GC–MS analyses were carried out on a Hewlett-Packard 5890 chromatograph interfaced to a HP 5970 mass spectrometer (EI, 70 eV).

Determination of Formation Constants of the EDA Complexes. In a typical experiment, a 2-mL aliquot of a standard stock solution of tropylium tetrafluoroborate (5 mM) in acetonitrile was placed in a 1-cm quartz cuvette. A known amount of arene was added in increments, and the absorbance changes were measured at the absorption maxima as well as at two other wavelengths close to the absorption maxima (see Figure 3). From a plot of $[C_7H_7^+BF_4^-]/A_{CT}$ against $[\text{arene}]^{-1}$, consisting of at least six data points, the slope was estimated as $(K\epsilon_{CT})^{-1}$ and the intercept as ϵ_{CT}^{-1}.[23] In the case of hexamethylbenzene and anthracene, owing to the limited solubility of these arenes in acetonitrile, the following procedure was adopted. To a 2-mL stock solution containing 3 mM hexamethylbenzene in acetonitrile contained in a 1-cm quartz curvette, a known amount of crystalline tropylium tetrafluoroborate was added in increments, and the absorbance changes of the CT band was measured. Similarly, in the case of anthracene, a solution containing 5 mM anthracene in acetonitrile was used. From a plot of $[\text{arene}]/A_{CT}$ against $[C_7H_7^+BF_4^-]^{-1}$, the slope was estimated as $(K\epsilon_{CT})^{-1}$ and the intercept as ϵ_{CT}^{-1}. The estimated errors in the values of K and ϵ determined were 5–15%, as judged by the saturation fraction[65] of 0.08–0.17 at the concentrations of arene donors and the tropylium acceptor used in this study.

Measurement of Charge-Transfer Spectra of Solid EDA Complexes. The charge-transfer spectra of the solid EDA complexes of various aromatic donors with tropylium salts were measured on a neutral alumina matrix. Samples were prepared by grinding together a mixture of 0.2 mmol of the arene, 0.2 mmol of the tropylium salt and neutral alumina (1 g) (6–8% of the mixture on alumina). Upon grinding, colors characteristic of the EDA complexes developed. Spectra were measured in a circular quartz cell against an alumina disk, as the reference. In the case of the EDA complex from naphthalene and tropylium tetrafluoroborate, the spectrum measured on alumina matrix was identical with that measured on a silica gel matrix, though the intensity of the CT band was higher on silica gel matrix. Similar procedure using Celite as the solid support was unsuccessful, and the characteristic color of the EDA complex did not appear upon grinding a mixture of naphthalene, tropylium tetrafluoroborate, and Celite.

Isolation of Crystalline EDA Complexes of Arenes with Tropylium Salts. The following tropylium tetrafluoroborate, hexafluoroarsenate, hexafluoroantimonate, and hexachloroantimonate salts were employed as follows. (a) In CH_3CN by diffusion of another nonpolar solvent: In a typical experiment, a mixture of the arene (0.2 mmol) and the tropylium salt (0.2 mmol) was dissolved in a minimum amount of acetonitrile (1–3 mL) in a test tube. The tube containing the colored solution of the EDA complex was suspended inside a large flask containing one of the following solvents: CH_2Cl_2, ether, CCl_4, hexane. The flask was closed, and the system was allowed to stand at room temperature. Under these conditions after 2–3 h only a colorless crystalline solid was deposited on the walls of the tube, which was identified as the tropylium salt. The following arenes were examined by this method, and in all cases only the tropylium salt crystallized from solution: hexamethylbenzene, mesitylene, anthracene, naphthalene, pyrene, phenanthrene, 9-methylanthracene, and 1,4-dimethylnaphthalene. (b) In liquid sulfur dioxide: In a typical experiment, a mixture of the arene (0.2 mmol) and the tropylium salt (excluding the hexachloroantimonate salt) was dissolved in a minimum amount of liquid sulfur dioxide (anhydrous, Matheson) at −5 to 0 °C, and the solution was cooled to −78 °C in a dry ice–acetone slurry. Under these conditions, solutions containing hexamethylbenzene, naphthalene, anthracene, and 9-methylanthracene merely yielded the corresponding crystalline arene. The characteristically colored EDA complexes did not separate from solution under these conditions. When the solution was evaporated very slowly to dryness, the individual colorless components crystallized (except the yellow 9-methylanthracene). (c) In CH_3CN: A saturated solution containing the arene (2 mmol) and the tropylium salt (2 mmol) in acetonitrile was placed in a test tube that was then allowed to stand in the open air at room temperature. In the case of anthracene, 9-methylanthracene and hexamethylbenzene, slow evaporation over a period of 24–36 h yielded the corresponding arene as colorless crystalline solids. The colored EDA complexes from these arenes did not crystallize under these conditions. (d) Isolation of the tropylium EDA complexes of naphthalene donors: A solution containing tropylium hexafluoroantimonate (48 mg, 0.15 mmol) and 1,4-dimethylnaphthalene (100 μL, 0.65 mmol) in acetonitrile (~1.5 mL) was placed in a test tube and allowed to stand in the open air for 24–36 h. During this period, the slow evaporation of the solvent deposited orange crystals on the sides of the tube approximately 1 cm above the surface. The ^{1}H NMR spectrum of the isolated crystalline material in CD_3CN showed the presence of 1,4-dimethylnaphthalene and tropylium hexafluoroantimonate in precisely 1:1 molar ratio. The isolated crystalline material was unstable, and it decomposed to a yellow amorphous material in 2–3 h. Complete drying of the crystals in vacuo for 30 min also resulted in decomposition of the crystals. The crystals when left in contact with the mother liquor in an open test tube were stable for several days. However, when the tube was sealed, the crystalline material redissolved into the solution. The crystalline EDA complex prepared in this manner was suitable for X-ray crystallography (vide infra). The crystalline EDA complexes of naphthalene with tropylium hexafluoroantimonate (yellow) and tropylium hexachloroantimonate (red-orange) were also isolated by similar procedure. The isolated crystalline solids showed similar properties and were suitable for X-ray crystallography (vide infra). Attempts to grow crystals of the EDA complexes of naphthalene and dimethylnaphthalene with tropylium tetrafluoroborate and hexafluoroarsenate by a similar procedure were unsuccessful. In these cases, the solid material obtained was colorless.

X-ray Crystallography of Tropylium EDA Complexes. The EDA complex [naphthalene, $C_7H_7^+SbCl_6^-$] obtained as a large, dark orange faceted column having approximate dimensions 0.48 × 0.28 × 0.17 mm was mounted on a glass fiber in a random orientation on a Nicolet

(63) Conrow, K. *Organic Synthesis*; Wiley: New York, 1973; Collect. Vol. V, 1138.

(64) Dauben, H. J.; Honnen, C. R.; Harmon, K. M. *J. Org. Chem.* **1960**, *25*, 1442.

(65) (a) Deranleau, D. A. *J. Am. Chem. Soc.* **1969**, *91*, 4044, 4050. (b) See also: Person, W. B. *J. Am. Chem. Soc.* **1965**, *87*, 167.

R3m/V automatic diffractometer. Since the material was seen to exhibit slow decomposition over time when removed from solvent, the sample crystal was coated with a thin shell of epoxy to retard solvent loss. The radiation used was Mo Kα monochromatized (λ = 0.71073 Å) by a highly ordered graphite crystal. Final cell constants, as well as other information pertinent to data collection and refinement, are listed in Table VI. The Laue symmetry was determined to be *mmm*, and from the systematic absences noted the space group was shown to be either $P2_1mn$, $Pm2_1n$, or *Pmmn*. Intensities were measured using the θ–2θ scan technique, with the scan rate depending on the count obtained in rapid prescans of each reflection. Two standard reflections were monitored after every 2 h or every 100 data collected, and these showed no significant decay. In reducing the data, Lorentz and polarization corrections were applied, as well as an empirical absorption correction based on ψ scans of 10 reflections having χ values between 70 and 90°. The unitary structure factors displayed acentric statistics, but since the analogous SbF_6 structure had been shown to crystallize in space group *Pmmn*, this centrosymmetric alternative was initially assumed. Despite several attempts using Patterson and direct methods, no solution for the structure could be found. Therefore, the space group was switched to $Pm2_1n$. Again, however, all attempts to solve the structure failed, and so finally space group $P2_1mn$ was tried. A difference Fourier map phased on the initial Patterson solution now gave a plausible model, although it was substantially different from that found for the previously determined SbF_6^- analogue. In this case, the cation and anion were both ordered on mirror sites, while the naphthalene was quite heavily disordered across two positions related by the mirror. Hydrogens were added at ideal calculated positions and constrained to riding motion, with fixed isotropic temperature factors. At this point, the data and atomic coordinates were converted to the conventional setting of $Pmn2_1$. The cation and anion atoms were refined anisotropically; however, due to the disorder the naphthalene was kept isotropic. The rigid body model used to refine the naphthalene (using 50% population factors for all atoms) was that of the ordered molecule found in the SbF_6^- refinement. In the early stages of least squares, the tropylium was refined as a rigid body consisting of $^1/_2$ ring anchored on the mirror at C11. When the naphthalene disorder was properly accounted for, the tropylium atoms were released to refine individually, at which point the ring began to deviate substantially from planarity, approaching a chair configuration. Since the atom most deviant from the plane, C11, was in a unique position with respect to the adjacent disordered naphthalene sites, this model was retained in the final refinement. It was uncertain, however, whether the tropylium was indeed nonplanar or whether the heavy disorder in the crystal structure had compromised the accuracy of the atomic coordinates slightly at this site. Since the compound crystallized in noncentrosymmetric, enantiomorphic space group, the inverse structure was also refined and showed significantly higher *R* values. Thus, the reported structure was presumed to represent the correct sense of polar direction involved. After all shift/esd ratios were less than 0.4, convergence was reached at the agreement factors listed in Table VI. The only unusually high correlations noted between any of the variables in the last cycle of full-matrix least-squares refinement were between the positional and thermal parameters of C13 and C14. The final difference density map showed a maximum peak of about 0.5 e A^{-3}. All calculations were made using the SHELXTL PLUS series of crystallographic programs.[66]

The EDA complex [1,4-dimethylnaphthalene, $C_7H_7^+SbF_6^-$] obtained as a very large, reddish orange block having approximate dimensions 0.62 × 0.56 × 0.48 mm after treatment with epoxy cement was mounted on a glass fiber as described above. The Laue symmetry was determined to be $2/m$, and from the systematic absences noted the space group was shown to be either $P2_1$ or $P2_1/m$. The unitary structure factors displayed acentric statistics, and space group $P2_1$ was assumed from the outset. The structure was solved by use of the SHELXTL Patterson interpretation program, which revealed the position of the Sb atom. The remaining non-hydrogen atoms were located in subsequent Fourier syntheses. The usual sequence of isotropic and anisotropic refinement was followed, after which all hydrogens were entered in ideal calculated positions and constrained to riding motion, with fixed isotropic temperature factors. The two methyl groups were treated as rigid bodies and allowed to rotate freely about the C–C bonds. The possibility of space group $P2_1/m$ was ruled out by the positioning of the tropylium ions, which would have to be heavily disordered if a mirror plane perpendicular to *b* were added. Although the compound crystallized in a noncentrosymmetric, enantiomorphic space group, the *R* values for the separate refinements of the two possible motif chiralities showed essentially no difference. No other attempt was made to determine the absolute sense of direction of the 2_1 screw axis. After all shift/esd ratios were less than 0.2, convergence was reached at the agreement factors listed in Table VI.

The EDA complex [naphthalene, $C_7H_7^+SbF_6^-$] obtained as a large, bright lemon yellow triangular plate having approximate dimensions 0.58 × 0.40 × 0.12 mm was covered with a thin coating of epoxy to retard solvent loss and mounted on a glass fiber in a manner described above. The Laue symmetry was determined to be *mmm*, and from the systematic absences noted the space group was shown to be either $P2_1mn$, $Pm2_1n$, or *Pmmn*. Since all of the molecules involved have internal *mm*2 symmetry, space group *Pmmn* was initially assumed. The structure was solved by use of the SHELXTL Patterson interpretation program, which revealed the position of the Sb atom. The remaining non-hydrogen atoms were located in subsequent difference Fourier syntheses, with much difficulty since both the cation and anion are massively disordered. At this point the space group was changed to the noncentrosymmetric equivalent, and additional atoms were generated to fill out the asymmetric unit. The heavy disorder remained, however, and very high correlations were noted between all of the mirror-related atoms. Thus, it was assumed that the space group was indeed *Pmmn* and that the disordered model was correct. The paucity of observed data from such a large sample crystal also supported the notion of heavy disorder. The naphthalene molecule was found to be ordered about an *mm*2 site such that the central C–C bond lay within one mirror plane while being perpendicular to the other. The disordered tropylium cation was found to occupy another *mm*2 site, with the ring bisected by one mirror and disordered by the perpendicular mirror. The most efficient way to refine this model was to use the tropylium fragment found in a tetraphenylborate salt,[67] which also was bisected by a mirror. This unit with attached hydrogens was refined as a rigid body anchored to one mirror at C4, with a single-variable isotropic temperature factor for all the carbons and a single-nonvariable isotropic temperature factor for the hydrogens. The net result was essentially a 14-membered ring, with all carbons virtually equidistant from their neighbors. It was impossible to ascertain whether this indicated two distinct orientations or whether it simply provided a good model for a diffuse toroid of electron density caused by complete disorder. The SbF_6 anion was quite severely disordered about another *mm*2 site. So many different orientations of the octahedron were involved that the weight of some of the F positions reduced them to essentially refining as hydrogens. Therefore, rather strict Sb–F distance constraints had to be employed to prevent the fluorines from "wandering". In order to get an approximation of the true populations of the F sites, each atom was refined with a fixed isotropic temperature factor of 0.11 while the populations varied. These refined values were then rounded off to the nearest $^1/_{12}$ for simplicity and held fixed for the remainder of the refinement while the single temperature factor was allowed to vary. The final population factors used for F1–F6 were $^1/_{12}$, $^1/_{12}$, $^1/_2$, $^1/_6$, $^1/_6$, and $^1/_2$, respectively. After all shift/esd ratios were less than 0.5, convergence was reached at the agreement factors listed in Table VI.

Time-Resolved Spectroscopy of the Charge-Transfer Excitation of Arene–Tropylium Tetrafluoroborate Complexes. The transient intermediates formed during the charge-transfer excitation of the EDA complexes of arenes and tropylium tetrafluoroborate were examined on the picosecond time scale. Time-resolved differential absorption spectra were obtained using a laser flash system that utilized the 532-nm second harmonic 30-ps (fwhm) pulses from a Quantel YG402 mode-locked Nd^{3+}:YAG laser as the excitation source (~10 mJ/pulse).[68] This wavelength corresponded to the excitation of only the charge-transfer band of the EDA complexes (see Figure 1). The analyzing beam was produced by passing the fundamental (1064 nm) through a solution consisting of a 1:1 mixture (v/v) of D_2O and H_2O in a 10-cm cuvette to generate a pulse of white light. The emergent white light has been measured to be a reasonably uniform continuum in the region 450–750 nm. Temporal measurements were made by varying the path length of the second harmonic with respect to the fundamental. The spectrograph was calibrated using the 532-nm band of the excitation pulse as well as the 436- and 546-nm lines from a low-pressure mercury lamp. The correction for the group velocity dispersion of this 30-ps laser system was negligible since the spectrometer calibration at 532 nm (laser pulse) and at 436/546 nm (Hg lines) showed a linear spectral dispersion. Measurements were made at times less than and greater than the maximum absorbance for the transient, such that t_0 could be determined as the time at which the absorbance due to the transient had reached its half-maximum. Spectra were measured at each time setting by averaging data from 30 individual pulses. The decay kinetics of the transients were

(66) Sheldrick, G. M *SHELXTL PLUS Programs for Crystal Structure Determination*; Nicolet XRD Corp.: Madison, WI, 1987.

(67) Bockman, T. M.; Kochi, J. K., unpublished results.

(68) See: Atherton, S. J.; Hubig, S. M.; Callan, T. J.; Duncanson, J. A.; Snowden, P. T.; Rodgers, M. A. J. *J. Phys. Chem.* **1987**, *91*, 3137. The incident intensity of the laser pulse was varied with wire-mesh screens; in the energy regime 0.013–0.16 mJ mm^{-2}, the signal intensities were linear with the laser pulse energies.

obtained by uniformly treating the data for first-order kinetics. The first-order rate constant thus obtained was reproducible to within ±25%.

Time-Resolved Absorption Spectra in the Microsecond to Nanosecond Time Regimes. The charge-transfer excitation of the EDA complexes from electron-rich arenes such as 9,10-dimethylanthracene and 1-methoxyanthracene with tropylium tetrafluoroborate did not show transient intermediates on the picosecond time scale. Thus, the time-resolved spectral studies of the CT excitation of the EDA complexes from these donors were examined on the microsecond to nanosecond time scales in a laser flash system consisting of a Quantel YG580-10 Q-switched Nd_3^+:YAG laser with a pulse width of 10 ns (fwhm). The 1064-nm pulse was frequency doubled with a KDP crystal and separated from the residual 1064 beam with a dichroic mirror to obtain 532-nm pulses of 160–170 mJ/shot. The laser intensity was attenuated using wire-mesh filters (50 and 30% transmittance with energy outputs of 75 and 50 mJ, respectively, at 532 nm). The interrogating beam consisted of the output from a 150-W xenon lamp in an Oriel lamp housing with an Aspherab UV-grade condensing lens. The probe beam was focused onto the sample, and then the emerging beam from the sample was focused onto an Oriel 77250 monochromator. A Hamamatsu R928NM photomultiplier tube attached to the exit slit of the monochromator served as the detector. The timing of the sequence for the excitation and probing of the sample was controlled by a Kinetic Instruments sequence generator and laser controller. Data acquisition and digitization were performed with a Tektronix 7104 oscilloscope in conjunction with a Tektronix C101 video camera and Tektronix DCS01 software. The data processing employed a AT&T 6300-plus computer using the ASYST 2.0 software. The charge-transfer excitation at 532 nm of the EDA complexes from 9,10-dimethylanthracene and 1-methoxyanthracene with a 10-ns laser pulse did not show transient intermediates in the interval from 200 ns up to 1 ms.

Charge-Transfer Cycloreversion of Anthracene and 9-Methylanthracene Dimers. The cycloreversion of the dianthracenes were examined in a 2:1 (v/v) mixture of methylene chloride and acetonitrile to accommodate the solubility of both tropylium tetrafluoroborate and the anthracene dimers. The cycloreversion of anthracene dimer was measured subsequent to the exposure of the solution containing 1.0 mM of the dimer and 0.05 M tropylium tetrafluoroborate in 2 mL of solvent with the output from a 1-kW xenon–mercury lamp (Hanovia 977B0010) that was focused through an aqueous IR filter followed by an Oriel monochromator (Model 77250). The quantum yields were obtained at 366 and 436 nm by measuring anthracene absorbance at 378 nm after dilution of an aliquot of the photolysate [λ_{max} = 378 nm, ϵ = 6750 M^{-1} cm^{-1} in 2:1 CH_2Cl_2/CH_3CN (v/v)]. Reinecke salt actinometry was used to calibrate the light intensities.[39] The measured quantum yields for cycloreversion obtained in three separate runs were Φ_p = 0.05, 0.02, and 0.03 at 366 nm and 0.02, 0.007, and 0.005 at 436 nm based on the 2:1 stoichiometry in eq 11.

The charge-transfer cycloreversion of the 9-methylanthracene dimer was similarly examined after the irradiation of a solution containing 2 mM of the dianthracene and 0.13 M tropylium tetrafluoroborate in 2 mL of solvent. The solution was irradiated at 420 nm with a focused beam from an Osram 450 W high-pressure xenon lamp that was equipped with an aqueous IR filter and an interference filter (10-nm band-pass, Edmund Scientific) as a monochromator. After irradiation for a specified period, an aliquot of the photolysate was diluted with 2:1 mixture of CH_2Cl_2 and CH_3CN, and the appearance of 9-methylanthracene was quantitatively monitored at 368 and 388 nm [λ_{max} = 368 nm, ϵ = 15 858 M^{-1} cm^{-1} and λ_{max} = 389 nm, ϵ = 15 360 M^{-1} cm^{-1} in a 2:1 mixture of CH_2Cl_2/CH_3CN]. Owing to the low absorbance of the CT band of the anthracene dimers with tropylium tetrafluoroborate, corrections were made for transmitted light at the wavelength of irradiation.[69] Owing to the high absorbance of the anthracene products at the monitoring wavelengths, the conversions were kept between 0.2 and 0.5%. The measured quantum yields for cycloreversion of the 9-methylanthracene dimer obtained in three separate runs were Φ_p = 0.03, 0.02, and 0.02 at 420 nm.

Charge-Transfer Isomerization of Hexamethyl(Dewar benzene). The solution to be irradiated was kept in a 1-cm precision quartz cell that was immersed in an acetone bath at −35 ± 5 °C in a Pyrex Dewar. Irradiation of the solution was performed with a focused beam from an Osram 450-W xenon lamp passed through an aqueous IR filter, followed by a 405-nm interference filter (10-nm band-pass, Edmund Scientific). The lamp intensity was calibrated with a Reinecke salt actinometer at 25 °C as described by Wegner and Adamson.[39] It was calculated to be 3.6 ± 0.5 × 10^{-8} einstein min^{-1} from three individual runs. Photolysis of the solution containing hexamethyl(Dewar benzene) and tropylium tetrafluoroborate in acetonitrile was carried out at −35 ± 5 °C by cooling the acetone bath with dry ice. Under these conditions, control experiments in the dark showed that the thermal isomerization of HMDB was negligibly slow during the duration of the photolysis as follows. A 3.0-mL aliquot of a stock solution containing 0.05 M hexamethyl(Dewar benzene) and 0.1 M tropylium tetrafluoroborate was photolyzed at −30 °C for typically 15–20 min with constant stirring. Another 3.0-mL aliquot of the stock solution was left in the dark at −30 °C, and it served as the blank. After photolysis, a 1.0-mL aliquot of each solution was diluted to 2.0 mL with precooled acetonitrile (−30 °C), and the absorption spectra were measured. The difference spectrum between the photolyzed and the blank solution showed a broad band with λ_{max} = 430 nm characteristic of the CT band of hexamethylbenzene and tropylium tetrafluoroborate. The concentration of the HMB was calculated from a calibration plot obtained as follows. The absorption spectrum of a solution containing 0.025 M HMDB and 0.05 M tropylium tetrafluoroborate in acetonitrile (at −30 °C) was measured and served as the blank spectrum. A known amount of HMB was added in increments and the spectrum of the mixture was remeasured. The difference in absorbance at 420, 430, and 440 nm between these spectra was plotted against the concentration of HMB. The linear plot consisted of six data points with a correlation coefficient of ≅0.996. The concentration of HMB formed during the photolysis was obtained from this plot knowing the difference in absorbance at 420, 430, and 440 nm of the photolyzed and the blank solution. The light intensity absorbed by the actinometer at room temperature and the HMDB solution at −30 °C was assumed to be the same. Corrections were made for any transmitted light in the latter solution. The quantum yields for the charge-transfer isomerization of HMDB from three individual runs were 3.8, 4.6, and 2.1.

Charge-Transfer Reactions of the EDA Complexes of Arenes with Tropylium Tetrafluoroborate. (a) Charge-transfer irradiation of 9,10-dimethylanthracene complex in the presence of pyridine bases: Addition of 2,6-di-*tert*-butylpyridine (183 mg, 9.5 mmol) to a purple solution of a mixture containing 9,10-dimethylanthracene (31 mg, 0.15 mmol) and tropylium tetrafluoroborate (26 mg, 0.15 mmol) in acetonitrile (3 mL) did not change the absorption spectrum (λ_{max} = 520 nm). The solution was irradiated with the output from a 500-W mercury lamp using a Corning cutoff filter CS-3-71 (λ < 480 nm). After irradiation for 6 h, the CT band persisted intact. The ^1H NMR spectrum of the crude mixture indicated the presence of only the starting materials. Similar experiments carried out with other donors, such as hexamethylbenzene, durene, and 9-methylanthracene, also showed no evidence of a photochemical reaction. In all cases the starting materials were recovered. When the reaction was carried out in the presence of 2,4,6-trimethylpyridine (1 eq), a slow thermal reaction occurred. Thus, the addition of 2,4,6-trimethylpyridine (20 μL, 0.15 mmol) to a deep red solution of 1,4-dimethylnaphthalene (23 μL, 0.15 mmol) and tropylium tetrafluoroborate (27 mg, 0.15 mmol) in acetonitrile (3 mL) caused the slow thermal bleaching of the CT band (λ_{max} = 440 nm) at room temperature. The reaction mixture was allowed to stand overnight, and solvent was removed. The ^1H NMR spectrum of the crude mixture indicated the complete disappearance of the resonances due to tropylium tetrafluoroborate (δ 9.30) and 2,4,6-trimethylpyridine (δ 6.79, 2.36, and 2.21). It also indicated the presence of 1,4-dimethylnaphthalene. The crude reaction mixture was washed with ether to remove 1,4-dimethylnaphthalene. The resulting pale yellow solid was identified as *N*-tropyl-2,4,6-trimethylpyridinium tetrafluoroborate. ^1H NMR (CD_3CN): δ 7.40 (s, 2 H), 6.66 (m, 2 H), 6.14 (m, 2 H), 5.45 (m, 2 H), 3.61 (m, 1 H), 2.60 (s, 6 H), 2.48 (s, 3 H). *N*-tropyl-2,4,6-trimethylpyridinium tetrafluoroborate obtained from the reaction of tropylium tetrafluoroborate with 2,4,6-trimethylpyridine in acetonitrile had an identical ^1H NMR spectrum. A mixture containing 2,4,6-trimethylpyridine (20 μL, 0.15 mmol), 1,4-dimethylnaphthalene (23 μL, 0.15 mmol), and tropylium tetrafluoroborate (27 mg, 0.15 mmol) in acetonitrile (3 mL) was irradiated at 0 °C using a 500-W high-pressure mercury lamp and a Corning cutoff filter (C-3-72; λ < 425 nm) for 3 h. Under these conditions the thermal reaction was absent. However, no photochemical reaction from the EDA complex was observed. (b) Decomposition of 9-(trimethylsiloxy)anthracene in the presence of tropylium tetrafluoroborate: When a purple solution containing 9-(trimethylsiloxy)anthracene (20 mg, 0.07 mmol) and tropylium tetrafluoroborate (13 mg, 0.07 mmol) in acetonitrile (3 mL) was allowed to stand at room temperature, the slow bleaching of the CT band (λ_{max} = 560 nm) was observed and a pale yellow solution was obtained after 10 h. The ^1H NMR spectrum of the reaction mixture showed the tropylium tetrafluoroborate to be intact (^1H NMR: δ 9.37). However, the resonances of 9-(trimethylsiloxy)-anthracene at δ 8.12 (m), 7.47 (m), and 0.38 (s) were gone. GC and GC–MS analysis of the mixture indicated the formation of anthrone and anthraquinone that were identified by comparison with authentic samples.

(69) Rabek, J. F. *Experimental Methods in Photochemistry and Photophysics*; Wiley: New York, 1982.

Acknowledgment. We thank S. J. Atherton, S. M. Hubig, and T. A. Albright for helpful advice, J. D. Korp for crystallographic assistance, and the Center for Fast Kinetic Research (under support from NIH Grant RR0886 and the University of Texas, Austin) for use of their picosecond laser facilities. We also acknowledge the National Science Foundation, the R. A. Welch Foundation, and the Texas Advanced Research Program for financial support and funds to construct the laser facility in Houston.

Supplementary Material Available: Tables of bond distances and angles and atomic coordinates and equivalent isotropic displacement parameters for tropylium EDA complexes (5 pages). Ordering information is given on any current masthead page.

The Total Synthesis of Avermectin A_{1a}

Samuel J. Danishefsky,* David M. Armistead, Francine E. Wincott, Harold G. Selnick, and Randall Hungate

Contribution from the Department of Chemistry, Yale University, New Haven, Connecticut 06511. *Received July 6, 1988*

Abstract: Key fragments for the total synthesis of the title compound were elaborated from D-ribose and D-glucose and coupled through a crossed aldol dehydration maneuver (**33** + **44** → **46**). An intramolecular variant of the Nozaki reaction (**47** → **48**) led to the all-critical oxahydrindene system. Disaccharide **66** was synthesized from fragments which were prepared by cyclocondensation reactions. Stereospecific coupling of **66** to aglycon **55** gave **67** and, eventually, avermectin A_{1a}.

Background and Synthetic Goals. The screening of microbially derived fermentation products for new antibacterial agents has provided for a fruitful collaboration among biology, chemistry, and medicine.[1] This type of multifaceted venture attained early prominence and success in the discovery and development of penicillins.[2] The possibilities of finding agents which might prove useful in other kinds of therapeutic applications are receiving increasing scrutiny.

It was in the course of investigating fermentation products of a broth derived from *Streptomyces avermitilis* MA-4680 that the avermectins were first encountered. An assay involving survival of mice infected with *Nematodirus dubuis* enabled a team of Merck scientists to discover anthelmentic activity of a high order from a soil sample from the Shizuaka Prefecture in Japan.[3] A collection of eight closely related compounds called avermectins was eventually separated into individual components. The delineation of the structures of these compounds relied heavily on a crystallographic determination of avermectin B_{1a} and avermectin B_{2a} aglycon.[4] From these firm bases, with extensive support via spectroscopic techniques and some chemical correlations, the structures of the eight compounds shown in Figure 1 could be deduced.[5]

The avermectins are active against two major classes of parasites, nematodes and arthropods. The mechanism of action appears to involve interferences with GABA-mediated muscular regulation. The quest for a detailed insight into the mechanism of action of this class of compounds and the evaluation of the therapeutic advantages of specific naturally occurring members, congeners, and semisynthetic mixtures (cf. ivermectins) is an important area of biomedical research.[6] The avermectins already enjoy extensive usage in animal (e.g. cattle, sheep, horses) health maintenance against a broad range of internal parasites.

The most promising targets of opportunity for structural manipulation of the activity profile have been in the carbohydrate region attached to C_{13} and in the unsaturation level of the spiroketal sector. Modifications of the oxahydrindene area and attempts at realizing avermectin activity via structures in which the macrolactone activity is simulated have been unrewarding.[7]

Not surprisingly, the combination of the novelty of the molecular structure of these compounds, their already demonstrated commercial importance, and the possibilities for discovery of new therapeutic uses, including human application, have engendered significant interest in the synthesis of avermectins.[8] Two important milestones in this regard were achieved by Smith and Williams, who independently reported the syntheses of milbemycin A_5.[9-11] A variety of sequences for the synthesis of the spiroketal section have been demonstrated.[12] More difficult has been the matter of a facile assembly of the oxahydrindene moiety.[13] Of late, some promising advances in this regard have been recorded.

Several important breakthroughs in charting a comprehensive strategy for the total synthesis of the avermectins have been achieved by Hanessian and co-workers. These studies established routes to the optically pure spiroketal of the avermectin 1a series

(1) Fisher, M. H.; Mrozik, H. *Macrolide Antibiotics*; Academic Press: New York, 1984; 553.
(2) Sheehan, J. C. *The Enchanted Ring*; MIT Press: Cambridge, 1982.
(3) Burg, R. W.; et al. *Antimicrob. Agents Chemother.* **1979**, *15*, 361.
(4) Springer, J. P.; Arison, B. A.; Hirshfield, J. M.; Hoogsteen, K. *J. Am. Chem. Soc.* **1981**, *103*, 4221.
(5) Albers-Schönberg, G.; Arison, B. H.; Chabala, J. C.; Douglas, A. W.; Eskola, P.; Fisher, M. H.; Lusi, A.; Mrozik, H.; Smith, J. L.; Tolman, R. L. *J. Am. Chem. Soc.* **1981**, *103*, 4216.
(6) Fisher, M. H. *Recent Advances in the Chemistry of Insect Control*; Janes, N. F., Ed.; Royal Society of Chemistry: London, 1985; p 53 and references therein.
(7) (a) Mrozik, H.; Eskola, P.; Fisher, M. H., Egerton, J. R.; Cifelli, S.; Ostlind, D. A. *J. Med. Chem.* **1982**, *25*, 658. (b) Chabala, J. C.; Mrozik, H.; Tolman, R. L.; Eskola, P.; Lusi, A.; Peterson, L. H.; Woods, M. F.; Fisher, M. H.; Cambell, W. C.; Egerton, J. R., Ostlind, D. A. *J. Med. Chem.* **1980**, *23*, 1134.
(8) For a recent review of related milbemycin syntheses, see: Davies, H. G.; Green, R. H. *Nat. Prod. Rep.* **1986**, 87.
(9) Smith, A. B., III; Schow, S. R.; Bloom, J. D.; Thompson, A. S.; Winzenburg, K. N. *J. Am. Chem. Soc.* **1982**, *104*, 4015.
(10) Schow, S. R.; Bloom, J. D.; Thompson, A. S. Winzenburg, K. N.; Smith, A. B., III *J. Am. Chem. Soc.* **1986**, *108*, 2662.
(11) Williams, D. R.; Barner, B. A.; Nishitani, K.; Phillips, J. G. *J. Am. Chem. Soc.* **1982**, *104*, 4708.
(12) For previous syntheses of milbemycin and avermectin spiroketals, cf. interalia: (a) Street, D. A.; Kocienski, P.; Campbell, S. F. *J. Chem. Soc., Chem. Commun.* **1985**, 1326. (b) Baker, R.; Boyes, R. H. O.; Broom, D. M. P.; Devlin, J. A.; Swain, C. J. *Ibid.* **1983**, 829. (c) Baker, R.; Swain, C. J.; Head, J. C. *Ibid.* **1985**, 309. (d) Hanessian, S.; Ugolini, A.; Therien, M. *J. Org. Chem.* **1983**, *48*, 4427. (e) Culshaw, D.; Grice, P.; Ley, S. V.; Strange, G. A. *Tetrahedron Lett.* **1985**, *26*, 5837. (f) Ardisson, J.; Férézou, J. P.; Julia, M.; Lenglet, L.; Pancrazi, A. *Tetrahedron Lett.* **1987**, *28*, 1997. (g) Attwood, S. V.; Barrett, A. G. M.; Carr, R. A. E.; Richardson, G. *J. Chem. Soc., Chem. Commun.* **1986**, 479.
(13) For synthetic studies related to the oxahydrindrene portion of the avermectins, see: (a) Jung, M. E.; Street, L. J. *J. Am. Chem. Soc.* **1984**, *106*, 8327. (b) Kozikowski, A. P.; MaloneyHuss, K. E. *Tetrahedron Lett.* **1985**, *26*, 5759. (c) Prashad, M.; Fraser-Reid, B. *J. Org. Chem.* **1985**, *50*, 1564. (d) Crimmins, M. T.; Lever, J. G. *Tetrahedron Lett.* **1986**, *27*, 291. (e) Ireland, R. E.; Obrecht, D. M. *Helv. Chim. Acta* **1986**, *69*, 1273. (f) Hanessian, S.; Beaulieu, P.; Dubé, D. *Tetrahedron Lett.* **1986**, *27*, 5071. (g) Barrett, A. G. M.; Capps, N. K. *Tetrahedron Lett.* **1986**, *27*, 5571. (h) Jung, M. E.; Street, L. H.; Usui, Y. *J. Am. Chem. Soc.* **1986**, *108*, 6810. (i) Ardisson, J.; Ferezou, J. P.; Julia, M.; Pancrazi, A. *Tetrahedron Lett.* **1987**, *28*, 2001.

0002-7863/89/1511-2967$01.50/0